Geosci. Model Dev., 9, 4405–4437, 2016
www.geosci-model-dev.net/9/4405/2016/
doi:10.5194/gmd-9-4405-2016
© Author(s) 2016. CC Attribution 3.0 License.

Geoscientific Model Development
Open Access
EGU

Terrestrial ecosystem process model Biome-BGCMuSo v4.0: summary of improvements and new modeling possibilities

Dóra Hidy[1], Zoltán Barcza[2], Hrvoje Marjanović[3], Maša Zorana Ostrogović Sever[3], Laura Dobor[2,14], Györgyi Gelybó[4], Nándor Fodor[5], Krisztina Pintér[1], Galina Churkina[6,15], Steven Running[7], Peter Thornton[8], Gianni Bellocchi[9], László Haszpra[10,13], Ferenc Horváth[11], Andrew Suyker[12], and Zoltán Nagy[1]

[1]MTA-SZIE Plant Ecology Research Group, Szent István University, Páter K. u.1., 2103 Gödöllő, Hungary
[2]Department of Meteorology, Eötvös Loránd University, Pázmány P. sétány 1/A., 1117 Budapest, Hungary
[3]Croatian Forest Research Institute, Department for Forest Management and Forestry Economics, Cvjetno naselje 41, 10450 Jastrebarsko, Croatia
[4]Institute for Soil Sciences and Agricultural Chemistry, Centre for Agricultural Research, Hungarian Academy of Sciences, Herman O. út 15., 1163 Budapest, Hungary
[5]Agricultural Institute, Centre for Agricultural Research, Hungarian Academy of Sciences, Brunszvik u. 2., 2462 Martonvásár, Hungary
[6]Institute for Advanced Sustainability Studies e.V., Berliner Strasse 130, 14467 Potsdam, Germany
[7]Numerical Terradynamic Simulation Group, Department of Ecosystem and Conservation Sciences University of Montana, Missoula, MT 59812, USA
[8]Climate Change Science Institute/Environmental Sciences Division, Oak Ridge National Laboratory, Oak Ridge, TN 37831, USA
[9]UREP, INRA, 63000 Clermont-Ferrand, France
[10]Hungarian Meteorological Service, P.O. Box 39, 1675 Budapest, Hungary
[11]Institute of Ecology and Botany, Centre for Ecological Research, Hungarian Academy of Sciences, Alkotmány u. 2-4., 2163 Vácrátót, Hungary
[12]School of Natural Resources, University of Nebraska-Lincoln, 806 Hardin Hall, Lincoln, NE 68588, USA
[13]Geodetic and Geophysical Institute, MTA Research Centre for Astronomy and Earth Sciences, Csatkai Endre utca 6-8, 9400 Sopron, Hungary
[14]Czech University of Life Sciences, Faculty of Forestry and Wood Sciences, Department of Forest Protection and Entomology, Kamýcká 129, 165 21 Prague 6, Czech Republic
[15]Geography Department, Humboldt University of Berlin, Berlin, Germany

Correspondence to: Dóra Hidy (dori.hidy@gmail.com)

Received: 18 April 2016 – Published in Geosci. Model Dev. Discuss.: 13 May 2016
Revised: 7 October 2016 – Accepted: 7 November 2016 – Published: 7 December 2016

Abstract. The process-based biogeochemical model Biome-BGC was enhanced to improve its ability to simulate carbon, nitrogen, and water cycles of various terrestrial ecosystems under contrasting management activities. Biome-BGC version 4.1.1 was used as a base model. Improvements included addition of new modules such as the multilayer soil module, implementation of processes related to soil moisture and nitrogen balance, soil-moisture-related plant senescence, and phenological development. Vegetation management modules with annually varying options were also implemented to simulate management practices of grasslands (mowing, grazing), croplands (ploughing, fertilizer application, planting, harvesting), and forests (thinning). New carbon and nitrogen pools have been defined to simulate yield and soft stem development of herbaceous ecosystems. The model version containing all developments is referred to as Biome-BGCMuSo (Biome-BGC with multilayer soil module; in this paper, Biome-BGCMuSo v4.0 is documented).

Published by Copernicus Publications on behalf of the European Geosciences Union.

Case studies on a managed forest, cropland, and grassland are presented to demonstrate the effect of model developments on the simulation of plant growth as well as on carbon and water balance.

1 Introduction

The development of climate models has led to the construction of Earth system models (ESMs) with varying degrees of complexity where the terrestrial carbon cycle is included as a dynamic sub-model (Ciais et al., 2013). In some of the ESMs, the atmospheric concentration of carbon dioxide (CO_2) is no longer prescribed by the emission scenarios but it is calculated dynamically as a function of anthropogenic CO_2 emission and the parallel ocean and land surface carbon uptake. Focusing specifically on land surface, the carbon balance of terrestrial vegetation can be quantified by state-of-the-art biogeochemical models and are integral parts of the ESMs.

At present, there is no consensus on the future trajectory of the terrestrial carbon sink (Fig. 6.24 in Ciais et al., 2013; see also Friedlingstein et al., 2014). Some ESMs predict saturation of the land carbon sink in the near future while others show that the uptake will stay on track with the increasing CO_2 emission. This means a considerable uncertainty is related to the climate–carbon cycle feedback (Friedlingstein et al., 2006; Friedlingstein and Prentice, 2010). The wide range of model data related to the land carbon sink means that the current biogeochemical models have inherent uncertainties which must be addressed.

Biogeochemical models need continuous development to include empirically discovered processes and mechanisms, e.g., acclimation processes describing the dynamic responses of plants to the changing environmental conditions (Smith and Dukes, 2012), regulation of stomatal conductance under elevated CO_2 concentration (Franks et al., 2013), drought effect on vegetation functioning (van der Molen et al., 2011), soil moisture control on ecosystem functioning (Yi et al., 2010), and other processes. Appropriate description of human intervention is also essential to adequately quantify lateral carbon fluxes and net biome production (Chapin et al., 2006). Staying on track with the new measurement-based findings is a challenging task but necessary to improve our ability to simulate the terrestrial carbon cycle more accurately.

The process-based biogeochemical model Biome-BGC is the focus of this study. The model was developed by the Numerical Terradynamic Simulation Group (NTSG), at the University of Montana (http://www.ntsg.umt.edu/project/biome-bgc), and is widely used to simulate carbon (C), nitrogen (N), and water fluxes of different terrestrial ecosystems such as deciduous and evergreen forests, grasslands, and shrublands (Running and Hunt, 1993; Thornton, 1998; Thornton et al., 2002; Churkina et al., 2009; Hidy et al., 2012).

Biome-BGC is one of the earliest biogeochemical models that include an explicit N cycle module. It is now clear that climate–carbon cycle interactions are affected by N availability and the CO_2 fertilization effect can be limited by the amount of N in ecosystems (Friedlingstein and Prentice, 2010; Ciais et al., 2013). Therefore, the explicit simulation of the N cycle is an essential part of these biogeochemical models (Thornton et al., 2007; Thomas et al., 2013).

Several researchers used and modified Biome-BGC in the past. Without being exhaustive, here we review some major applications on forest ecosystems, grasslands, croplands, urban environment, and we also list studies that focused on the spatial application of the model on regional and global scales.

Vitousek et al. (1988) studied the interactions in forest ecosystems such as succession, allometry, and input–output budgets using Biome-BGC. Nemani and Running (1989) tested the theoretical atmosphere–soil–leaf area hydrologic equilibrium of forests using satellite data and model simulation with Biome-BGC. Korol et al. (1996) tested the model against observed tree growth and simulated the 5-year growth increments of 177 Douglas fir trees growing in uneven-aged stands. Kimball et al. (1997) used Biome-BGC to simulate the hydrological cycle of boreal forest stands. Thornton et al. (2002) improved the model to simulate harvest, replanting, and forest fire. Churkina et al. (2003) used Biome-BGC to simulate coniferous forest carbon cycle in Europe. Pietsch et al. (2003) developed Biome-BGC in order to take into account the effect of water infiltration from groundwater and seasonal flooding in forest areas. Bond-Lamberty et al. (2005) developed Biome-BGC-MV to enable simulation of forest species succession and competition between vegetation types. Vetter et al. (2005) used Biome-BGC to simulate the effect of human intervention on coniferous forest carbon balance. Schmid et al. (2006) assessed the accuracy of Biome-BGC to simulate forest carbon balance in central Europe. Tatarinov and Cienciala (2006) further improved the Biome-BGC facilitating management practices in forest ecosystems (including thinning, felling, and species change). Merganičová et al. (2005) and Petritsch et al. (2007) implemented forest management in the model including thinning and harvest. Bond-Lamberty et al. (2007a) implemented elevated groundwater effect on stomatal conductance and decomposition in Biome-BGC, and then simulated wildfire effects across a western Canadian forest landscape (Bond-Lamberty et al., 2007b). Chiesi et al. (2007) evaluated the applicability of Biome-BGC in drought-prone Mediterranean forests. Turner et al. (2007) used Biome-BGC to estimate the carbon balance of a heterogeneous region in the western United States. Ueyama et al. (2010) used the model to simulate larch forest biogeochemistry in east Asia. Maselli et al. (2012) used the model to estimate olive fruit yield in Tuscany, Italy. Hlásny et al. (2014) used Biome-BGC to sim-

ulate the climate change impacts on selected forest plots in central Europe.

Di Vittorio et al. (2010) developed Agro-BGC to simulate the functioning of C4 perennial grasses including a new disturbance handler and a novel enzyme-driven C4 photosynthesis module.

Wang et al. (2005) applied Biome-BGC to simulate cropland carbon balance in China. Ma et al. (2011) developed ANTHRO-BGC to simulate the biogeochemical cycles of winter crops in Europe, including an option for harvest and considering allocation to yield.

Trusilova and Churkina (2008) applied Biome-BGC to estimate the carbon cycle of urban vegetated areas.

Lagergren et al. (2006) used Biome-BGC to estimate the carbon balance of the total forested area in Sweden. Mu et al. (2008) used Biome-BGC to estimate the carbon balance of China. In the paper of Jochheim et al. (2009), forest carbon budget estimates were presented for Germany based on a modified version of Biome-BGC. Barcza et al. (2009, 2011) used Biome-BGC to estimate the carbon balance of Hungary. Eastaugh et al. (2011) used Biome-BGC to estimate the impact of climate change on Norway spruce growth in Austria. Biome-BGC was used within the CARBOEUROPE-IP project as well as in several studies exploiting the related European-scale simulation results (e.g., Jung et al., 2007a, b; Vetter et al., 2008; Schulze et al., 2009; Ťupek et al., 2010; Churkina et al., 2010).

Hunt et al. (1996) used Biome-BGC in a global-scale simulation and compared the simulated net primary production (NPP) with satellite-based vegetation index. Hunt et al. (1996) also used an atmospheric transport model coupled with Biome-BGC to simulate surface fluxes to estimate the distribution of CO_2 within the atmosphere. Churkina et al. (1999) used Biome-BGC in a global-scale multimodel intercomparison to study the effect of water limitation on NPP. Churkina et al. (2009) used Biome-BGC in a coupled simulation to estimate the global carbon balance for the present and up to 2030. Biome-BGC is used in the Multiscale synthesis and Terrestrial Model Intercomparison Project (MsTMIP) (Huntzinger et al., 2013; Schwalm et al., 2010) as part of the North American Carbon Program.

In spite of its popularity and proven applicability, the model development temporarily stopped at version 4.2. One major drawback of the model was its relatively poor performance in the simulation of the effect of management practices. It is also known that anthropogenic effects have a major role in the transformation of the land surface in large spatial scales (Vitousek et al., 1998). Some structural problems also emerged, like the simplistic soil moisture module (using one soil layer), lack of new structural developments (see, e.g., Smith and Dukes, 2012), problems associated with phenology (Hidy et al., 2012), and lack of realistic response of ecosystems to drought (e.g., senescence).

Our aim was to improve the model by targeting significant structural development, and to create a unified, state-of-the-art version of Biome-BGC that can be potentially used in Earth system models, as well as in situations where management and water availability play an important role (e.g., in semi-arid regions) in biomass production. The success and widespread application of Biome-BGC can be attributed to the fact that Biome-BGC strikes a great balance between process fidelity and tractability: it is relatively easy to use and run, even for non-specialists, but still yields interesting insights. The success can also be attributed to the open-source nature of the model code. Following this tradition, we keep the developed Biome-BGC open source. In order to support application of the model, a comprehensive user guide was also compiled (Hidy et al., 2015).

In the present work, the scientific basis of the developments is presented in detail, followed by verification studies in different ecosystems (forest, grassland, and cropland) to demonstrate the effect of the developments on the simulated fluxes and pools.

2 Study sites

Model developments were motivated by the need to improve model simulation for grasslands, croplands, and forests. Here, we demonstrate the applicability of the developed model at three sites on three different plant functional types characterized by contrasting management, climate, and site conditions.

2.1 Grassland/pasture

The large pasture near Bugacpuszta (46.69° N, 19.60° E; 111 m a.s.l.) is situated in the Hungarian Great Plain, covering an area of 1074 ha. The study site (2 ha) has been used as pasture for the last 150 years according to archive army maps from the 19th century. The soil surface is characterized by an undulating microtopography formed by winds within an elevation range of 2 m. The vegetation is highly diverse (species number over 80) dominated by *Festuca pseudovina* Hack. ex Wiesb., *Carex stenophylla* Wahlbg., *Cynodon dactylon* (L.) Pers., and *Poa* spp.

The average annual precipitation is 562 mm and the annual mean temperature is 10.4 °C. According to the FAO classification (Driessen et al., 2001) the soil type is chernozem with a rather high organic carbon content (51.5 g kg^{-1} for the 0–10 cm top soil; Balogh et al., 2011). The soil texture is sandy loamy sand (sand content 78 %, silt content 9 % in the 0–10 cm soil layer). The pasture belongs to the Kiskunság National Park and has been under extensive grazing by a Hungarian grey cattle herd in the last 20 years. Stocking density was 0.23–0.58 animal ha^{-1} during the 220-day grazing period between 2004 and 2012.

Carbon dioxide (CO_2) and latent heat flux (LHF) have been measured by the eddy-covariance (EC) technique. Continuous measurements began in 2003 and they are used in

this study as input and verification data (Nagy et al., 2007, 2011). The EC station has a measurement height of 4 m and is equipped with a CSAT3 (Campbell Scientific) sonic anemometer and a LI-7500 open-path infrared gas analyzer (IRGA; LI-COR Inc., Lincoln, NE, USA). Air temperature, relative humidity, precipitation, global radiation, and soil temperature are also monitored. Soil water content is measured by CS616 (Campbell Scientific, Shepshed, Leicestershire, UK) probes. Two probes were inserted horizontally at 3 and 30 cm depth and one was inserted vertically averaging the soil water content of the upper 30 cm soil layer. For model evaluation, measured soil water content at 30 cm depth was used.

Data processing includes spike detection and removal following Vickers and Mahrt (1997) and linear detrending to calculate fluctuations from the raw data. To avoid errors caused by the flow disturbance effect of the sensor heads, the correction proposed by van der Molen et al. (2004) was applied. The planar fit method (Wilczak et al., 2001) was used to correct for sonic anemometer tilt. Crosswind correction was applied for sensible heat flux calculation after Liu et al. (2001). The Webb–Pearman–Leuning correction (WPL; Webb et al., 1980) was used to consider the effect of fluctuations in air density on the fluxes. Frequency response corrections were applied after Moore (1986) to account for the damping effect of sensor line averaging, lateral separation between the IRGA and the sonic anemometer, and the limited time response of the sensors. The gap-filling and flux partitioning methods are based on the nonlinear function between photosynthetically active photon flux density (PPFD) and daytime CO_2 fluxes, and temperature and nighttime CO_2 fluxes (Reichstein et al., 2005).

2.2 C4 cropland

Three production-scale cropland measurement sites were established in 2001 at the University of Nebraska Agricultural Research and Development Center near Mead, Nebraska, USA, which are the part of the AmeriFlux (http://ameriflux.ornl.gov/) and the FLUXNET global network (http://fluxnet.ornl.gov/). Mead1 (41.17° N, 96.48° W; 361 m a.s.l.; 48.7 ha) and Mead2 (41.16° N, 96.47° W; 362 m a.s.l.; 52.4 ha) are both equipped with center pivot irrigation systems. Mead3 (41.18° N, 96.44° W; 362 m a.s.l.; 65.4 ha) relies on rainfall. Maize is planted each year at Mead1, while Mead2 and Mead3 are in a maize–soybean rotation.

On the Mead sites, the annual average temperature is 10.1 °C and the mean annual precipitation total is 790 mm. Soil at the site is deep silty clay loam consisting of four soil series: Yutan (fine–silty, mixed, superactive, mesic Mollic Hapludalfs), Tomek (fine, smectitic, mesic Pachic Argialbolls), Filbert (fine, smectitic, mesic Vertic Argialbolls), and Fillmore (fine, smectitic, mesic Vertic Argialbolls).

The CO_2 and energy fluxes are measured by an EC system using an omnidirectional three-dimensional sonic anemometer (model R3, Gill Instruments Ltd., Lymington, UK), an open-path infrared CO_2 / H_2O gas analyzer (model LI-7500: LI-COR Inc., Lincoln, NE, USA), and a closed-path CO_2 / H_2O system (model LI-6262: LI-COR Inc., Lincoln, NE, USA). The sensors were mounted 3 m above the ground when the canopy was shorter than 1 m, and later moved to a height of 6 m until harvest when maize was planted (Suyker et al., 2004; Verma et al., 2005).

Raw EC data processing included correction of fluxes for inadequate sensor frequency response (i.e., tube attenuation, sensor separation; Massman, 1991; Moore, 1986). Fluxes were adjusted for flow distortion (Nakai et al., 2006) and the variation in air density due to the transfer of water vapor (Webb et al., 1980; Suyker et al., 2003).

Air temperature and humidity were measured at 3.0 and 6.0 m height (Humitter50Y, Vaisala, Helsinki, Finland). PPFD (LI 190SA Quantum Sensor, LI-COR Inc., Lincoln, NE, USA), net radiation at 5.5 m height (Q*7.1, Radiation and Energy Balance Systems Inc., Seattle, WA, USA), and soil heat flux (0.06 m depth; Radiation and Energy Balance Systems Inc.) were also measured (Verma et al., 2005). Soil water content measured at 0.1 m depth was used in this study (ML2 Thetaprobe, Delta T Devices Ltd, Cambridge, UK).

Green leaf area index (LAI) was determined from destructive sampling. A LI-COR 3100 (LI-COR Inc., Lincoln, NE, USA) leaf area meter was used to measure sampled leaves. Each sampling was from six 1 m row samples from six parts of the field. Aboveground biomass was determined using destructive plant sampling. Plants were cut off at ground level, brace roots were removed, and plants were placed in fine mesh bags. Plants were dried to constant weight. Subsequently, the mass of green leaves, stems, reproductive organs, and senesced tissue was determined on a per-plant basis. Measured plant populations were used to convert from per-plant basis to a unit-ground-area basis.

The Mead1 site was under no-till management prior to the harvest of 2005. Currently, there is a fall conservation tillage for which approximately one-third of the crop residue is left on the surface. From 2010 to 2013, for a biomass removal study, management at Mead2 was identical to Mead1 (continuous maize, fall conservation tillage, etc.). Management settings of the simulations were based on site records. In this study, the Mead1 site is used for model evaluation.

2.3 Deciduous broad-leaved forest

The Jastrebarsko site (45.62° N, 15.69° E; 115 m a.s.l.) is a forest study site situated in a lowland oak forest that is part of the state-owned Pokupsko basin forest complex, located approximately 35 km southwest of Zagreb (Croatia). The forest compartment where the EC tower for CO_2 flux measurement is located was a 37-year-old mixed stand dominated by *Quercus robur* L. (58 %) accompanied by other tree species, namely *Alnus glutinosa* (L.) Gaertn. (19 %), *Carpinus betulus* L. (14 %), *Fraxinus angustifolia* Vahl. (8 %), and others

(1 %). *Corylus avellana* L. and *Crataegus monogyna* Jacq. are common in the understory. Oak forests in this area are managed in 140-year rotations. Stands are thinned once every 10 years ending with regeneration cuts during the last 10 years of the rotation (two or three), aimed at facilitating natural regeneration of the stand and continuous cover of the soil.

Annual mean temperature was 10.6 °C and average annual precipitation was 962 mm during the period of 1981–2010 (data from the National Meteorological and Hydrological Service for the Jastrebarsko meteorological station). The average annual depth to the groundwater ranges from 60 to 200 cm (Mayer, 1996). Groundwater level in a 4 m deep piezometer was measured weekly during the vegetation season from 2008 onwards. The forest is partly flooded with stagnating water during winter and early spring due to the heavy soil present at the site. Soil is generally Gleysol with low water conductivity (Mayer, 1996), and according to the World Reference Base for Soil Resources (WRB, 2006), it is classified as Luvic Stagnosol. The soil texture is dominantly clay with 18 % of sand and 28 % of silt fraction in the 0–30 cm top soil layer (Mayer, 1996).

Carbon dioxide and latent heat flux have been measured by the EC technique since September 2007 (Marjanović et al., 2011a, b). The measurement height at the time of installation was 23 m above ground (3–5 m above the top of the canopy). Since the forest stand grew, the measurement height was elevated to 27 m in April 2011. The EC system was made up of a sonic anemometer (81 000 V, R.M. Young, USA) and an open-path IRGA (LI-7500, LI-COR Inc., Lincoln, NE) with a sampling rate of 20 Hz. Meteorological measurements included soil temperature, incoming shortwave radiation, incoming and outgoing PPFD, net radiation, air temperature and humidity, soil heat flux, and total rainfall. Soil water content was measured at 0–30 cm depth using two time-domain reflectometers (Marjanović et al., 2011a).

Raw data processing of EC data was made using EdiRe Data Software (University of Edinburgh, United Kingdom) according to the methodology based on the EuroFlux protocol (Aubinet et al., 2000) with a further adjustment such as the WPL correction (Webb et al., 1980). Quality control was performed after Foken and Vichura (1996). Net ecosystem exchange (NEE) was obtained after taking into account the storage term which was calculated using a profile system designed to make sequential CO_2 concentration measurements (IRGA, SBA-4, PP Systems) from six heights in a 6 min cycle. Quality assessment and quality control was made according to Foken and Vichura (1996). Gap-filling of missing data and NEE flux partitioning to gross primary production (GPP) and total ecosystem respiration (TER) was made using online EC data gap-filling and flux partitioning tools (http://www.bgc-jena.mpg.de/~MDIwork/eddyproc/) using the method of Reichstein et al. (2005).

Jastrebarsko forest stand characteristics data include diameter at breast height (dbh) and volume distribution by tree species, weekly tree stem and annual height increment, tree mortality, phenology data, annual litterfall, litterfall C and N content, fine root biomass, net annual root-derived carbon input, soil texture, and carbon content (Marjanović et al., 2011b; Ostrogović, 2013; Alberti et al., 2014). Data were used either as input in modeling (e.g., groundwater level), for assessing some of the model parameters (e.g., phenology data) or model evaluation (e.g., EC fluxes, tree increment measurements).

3 Description of base model: Biome-BGC 4.1.1 MPI

Our model developments started before Biome-BGC 4.2 was published. The starting point was Biome-BGC v4.1.1 with modifications described in Trusilova et al. (2009). We refer to this model as Biome-BGC v4.1.1 MPI version (MPI refers to the Max Planck Institute in Jena, Germany) or original Biome-BGC. Biome-BGC v4.1.1 MPI version was developed from the Biome-BGC family of models (Thornton, 2000). Biome-BGC is the extension and generalization of the Forest-BGC model to describe different vegetation types including C3 and C4 grasslands (Running and Coughlan, 1988; Running and Gower, 1991; Running and Hunt, 1993; Thornton, 2000; White et al., 2000; Trusilova et al., 2009).

Biome-BGC uses a daily time step. The model is driven by daily values of minimum and maximum temperatures, precipitation, daytime mean global radiation, and daylight average vapor pressure deficit (VPD). In addition, Biome-BGC uses site-specific data (e.g., soil texture, site elevation, latitude), and ecophysiological data (e.g., maximum stomatal conductance, specific leaf area, C : N mass ratios in different plant compartments, allocation of related parameters) to simulate the biogeochemical processes of the given biome. The main simulated processes are photosynthesis, evapotranspiration, allocation, litterfall, and C, N, and water dynamics in the litter and soil (Thornton, 2000).

The three most important blocks of the model are the phenological, the carbon flux, and the soil flux block. The phenological block calculates foliage development and therefore affects the accumulation of C and N in leaf, stem (if present), root and consequently the amount of litter. In the carbon flux block, gross primary production of the biome is calculated using Farquhar's photosynthesis routine (Farquhar et al., 1980) and the enzyme kinetics model based on Woodrow and Berry (1988). Autotrophic respiration is separated into maintenance and growth respirations. In addition to temperature, maintenance respiration is calculated as the function of the N content of living plant pools, while growth respiration is a fixed proportion of the daily GPP. The soil block describes the decomposition of dead plant material (litter) and soil organic matter, N mineralization, and N balance in general (Running and Gower, 1991). The soil block uses the so-called converging cascade model (Thornton and Rosenbloom, 2005).

In Biome-BGC, the main parts of the simulated ecosystem are defined as plant, soil and litter. As Biome-BGC explicitly simulates the water, carbon and N balance of the soil–plant system, the most important pools include leaf (C, N, and water), fine root (C, N), soil (C, N, and water), and litter (C, N). C and N pools have additional sub-pools (i.e., so-called actual pools, storage pools, and transfer pools). The actual sub-pools are defined to store the amount of C and N that is available for growth on a given day. The storage sub-pools contain the amount of C and N that will appear during the next year's growing season (in this sense they are the virtualization of seeds or buds). The transfer sub-pools inherit the entire content of the storage pools at the end of a given year.

The model simulation has two phases. The first is the spinup simulation (or, in other words, the self-initialization or equilibrium run), which starts with a very low initial level of soil C and N and runs until a steady state is reached under the given climate in order to estimate the initial values of the state variables (Thornton, 2000; Thornton and Rosenbloom, 2005). In the second phase, the normal simulation uses the results of the spinup simulation as initial values for the C and N pools. This simulation is performed for a given predetermined time period.

4 Methodological results: model adjustments

Some improvements focusing primarily on the development of the model to simulate carbon and water balance of managed herbaceous ecosystems have already been published (Hidy et al., 2012). Previous model developments included structural improvements on soil hydrology and plant phenology. Additionally, management modules were implemented in order to provide more realistic fluxes for managed grasslands. We refer to this model version as the modified Biome-BGC (this is the predecessor of the current model).

Several developments have been made since the publication of the Hidy et al. (2012) study. The developments were motivated by multiple factors. Poor agreement of the modified Biome-BGC with available eddy covariance measurements made in Hungary over two grassland sites (see Hidy et al., 2012) clearly revealed the need for more sophisticated representation of soil hydrology, especially at the drought-prone, sandy Bugac site. Implementation and benchmarking of the multilayer soil module resulted in several additional developments related, e.g., to the N balance, soil temperature, root profile, soil water deficit effect on plant functioning, and decomposition of soil organic matter. Lack of management descriptors within the original Biome-BGC motivated the development of a broad array of possible management techniques covering typical grassland, cropland, and forest management practices. Modeling exercises within international projects revealed additional problems that needed a solution related, e.g., to stomatal conductance (Sándor et al., 2016). Recently published findings (e.g., simulation of temperature acclimation of respiration; Smith and Dukes, 2012) also motivated our work on model development. Addressing the known issues with the Biome-BGC model required diverse directions, but this was necessary due to the complex nature of the biogeochemical cycles of the soil–plant system. Our overarching aim was to provide a state-of-the-art biogeochemical model that is in the same league as currently available models, such as LPJmL, ORCHIDEE, CLM, JULES, CASA, and others.

The model that we present in this study is referred to as Biome-BGCMuSo (abbreviated as BBGCMuSo, where MuSo refers to a multilayer soil module). Currently, BBGC-MuSo has several versions but hereafter only the latest version (4.0) is discussed.

In this paper, we provide detailed documentation of all changes made in the model logic compared to the original model (Biome-BGC v4.1.1). Here, we briefly mention the previously published developments and we provide detailed descriptions concerning the new features. In order to illustrate the effect and the importance of the developments, model evaluations are presented for three contrasting sites equipped with EC measurement systems in Sect. 5.

Due to the modifications of the model structure and the implementation of the new management modules, it was necessary to modify the structure of the input and output files of the model. Technical details are discussed in the user guide of BBGCMuSo v4.0 (Hidy et al., 2015; http://nimbus.elte.hu/bbgc/files/Manual_BBGC_MuSo_v4.0.pdf).

We summarized the model adjustments in Table 1. Within the table, the implemented processes are grouped for clarity. Below, we document the adjustments in detail.

4.1 Multilayer soil

The predecessor of Biome-BGC (FOREST-BGC) was developed to simulate the carbon and water budgets of forests where soil moisture limitation is probably less important due to the deeper rooting zone. Therefore, its soil sub-model was simple and included only a one-layer budget model. Due to the recognized importance of soil hydrology on the carbon and water balance, state-of-the-art biogeochemical models include a multilayer soil module (e.g., Schwalm et al., 2015).

In order to improve the simulation quality of water and carbon fluxes with Biome-BGC, a seven-layer soil sub-model was implemented. Higher number of soil layers might be useful to better represent the soil profile in terms of soil texture and bulk density. This should be beneficial for sites with complex hydrology (see, e.g., the Jastrebarsko case study in Sect. 5.3). Additional layers also improve the representation of soil water content profile as the upper, thinner soil layers typically dry out more than the deeper layers, which affects soil and plant processes. As rooting depth can be quite variable, additional layers might support the proper representation of soil water stress on plant functioning. The seven layers provide an optimal compromise between simulation

Table 1. Summary of model adjustments. Group refers to major processes represented by collection of modules in Biome-BGCMuSo, while sub-group refers to specific features.

Group	Sub-group	Description
Multilayer soil	Thermodynamics	Two methods to calculate soil temperature layer by layer: logarithmic and the Ritchie (1998) method
	Hydrology	Calculation of soil water content and soil properties layer by layer New processes: percolation, diffusion, runoff, and pond water formation
	Root distribution	Calculation of root mass proportion layer by layer based on empirical function after Jarvis (1989)
	Nitrogen budget	Instead of uniform distribution, calculation of soil mineral nitrogen content layer by layer
	Soil moisture stress index	Soil moisture stress index based on normalized soil water content calculated layer by layer
	Senescence	Senescence calculation based on soil moisture stress index and the number of days since stress is present
	Decomposition and respiration	Maintenance root respiration flux is calculated layer by layer Limitation of soil moisture stress index
Management	Management modules	Mowing, grazing, harvest, ploughing, fertilization, planting, thinning, and irrigation Seven different events for each management activity can be defined per year, even in annually varying fashion
	Management-related plant mortality	Rate of the belowground decrease to the mortality rate of the aboveground plant material can be set optionally
Other plant-related processes	Phenology	Alternative model-based phenology Calculating start and end of vegetation period using heat sum index for growing season (extension of index in Jolly et al., 2005)
	Genetically programmed leaf senescence	Genetically programmed leaf senescence due to the age of the plant tissue
	New plant pools	Fruit and soft stem
	C_4 photosynthesis	Enzyme-driven C4 photosynthesis routine based on the work of Di Vittorio et al. (2010)
	Acclimation	Photosynthesis and respiration acclimation of plants, temperature-dependent Q_{10} (Smith and Dukes, 2012)
	LAI-dependent albedo	LAI-dependent albedo estimation based on the method of Ritchie (1998)
	Stomatal conductance regulation	CO_2 concentration is taken into account in stomatal conductance estimation based on the Franks et al. (2013)
Model run	Dynamic mortality	Ecophysiological parameter for whole-plant mortality fraction can be defined year by year
	Transient run	Optional third model phase to enable smooth transition from the spinup phase to the normal phase
	Possibility of land-use-change simulation	Avoiding frequent model crash in the case of different ecophysiological parameters set in spinup and normal simulations
Methane and nitrous oxide soil efflux	Unmanaged soils	Empirical estimation based on Hashimoto et al. (2011)
	Grazing and fertilization	Empirical estimation based on IPCC (2006) Tier 1 method

accuracy and computational cost. In accordance with the soil layers, we also defined new fluxes within the model. Note that in the Hidy et al. (2012) publication the developed Biome-BGC had only four soil layers, so the seven-layer module is an improvement.

The first layer is located at a depth of 0–10 cm, the second is at 10–30 cm, the third is at 30–60 cm, the fourth is at 60–100 cm, the fifth is at 100–200 cm, and the sixth is at 200–300 cm. The bottom (seventh, hydrologically and thermally inactive) layer is located at a depth of 300–1000 cm. The depth of a given soil layer is represented by the center

of the given layer. Below 5 m, the soil temperature can be assumed equal to the annual average air temperature of the site (Florides and Kalogirou, 2016). Furthermore, in the bottom layer we assume that soil water content (SWC) is equal to the field capacity (constant value) and soil mineral content has a small, constant value (1 kg N ha^{-1} within the 7 m deep soil column). The percolated water (and soluble N) to the bottom hydrologically inactive layer is a net loss, while the water (and soluble N) diffused upward from the bottom layer is a net gain for the simulated soil system.

Soil texture and soil bulk density can be defined by the user, layer by layer. If the maximum rooting zone (defined by the user) is greater than 3 m, the roots reach the constant boundary soil layer and water uptake can occur from that layer, as well. In previous BBGCMuSo model versions, the soil texture was constant with depth, and the maximum possible rooting depth was 5 m.

4.1.1 Soil thermodynamics

Since some of the soil processes depend on the actual soil temperature (e.g., decomposition of soil organic matter), it is necessary to calculate soil temperature for each active layer. Given the importance of soil temperature (e.g., Sándor et al., 2016), the soil module was also reconsidered in BBGCMuSo. The daily soil surface temperature is determined after Zheng et al. (1993). The basic equations are detailed in Hidy et al. (2012). An important modification in BBGCMuSo is that the average temperature of the top soil layer (with a thickness of 10 cm) is not equal to the above-mentioned daily surface temperature. Instead, temperature of the active layers is estimated based on an empirical equation with daily time steps.

Two optional empirical estimation methods are implemented in BBGCMuSo. The first is a simple method, assuming a logarithmic temperature gradient between the surface and the constant temperature boundary layer. This is an improvement compared to the modified Biome-BGC where a linear gradient was assumed. The second method is based on the soil temperature estimation method of the DSSAT model family (Ritchie, 1998) and the 4M model (Sándor and Fodor, 2012).

4.1.2 Soil hydrology

The C and the hydrological cycles of the ecosystems are strongly coupled due to interactions between soil moisture and stomatal conductance, soil organic matter decomposition, N mineralization, and other processes. Accurate estimation of the soil water balance is thus essential.

Among soil hydrological processes, the original Biome-BGC only takes into account plant uptake, canopy interception, snowmelt, outflow (drainage), and bare soil evaporation. We have added the simulation of runoff, diffusion, percolation, and pond water formation and enhanced the simulation of the transpiration processes in order to improve the soil water balance simulation. Optional handling of seasonally changing groundwater depth (i.e., possible flooding due to elevated water table) is also implemented. In the Hidy et al. (2012) study, only runoff, diffusion, and percolation were implemented (the simulation of these processes has been further developed since then). Pond water formation and simulation of groundwater movement are new features in BBGCMuSo 4.0.

Estimation of characteristic soil water content values

There are four significant characteristic points of the soil water retention curve: saturation, field capacity, permanent wilting point, and hygroscopic water. Beside volumetric SWC, soil moisture status can also be described by soil water potential (PSI; MPa). The Clapp–Hornberger parameter (B; dimensionless) and the bulk density (BD; g cm^{-3}), are also important in soil hydrological calculations (Clapp and Hornberger, 1978). Soil texture information (fraction of sand and silt within the soil; clay fraction is calculated by the model internally as a residual) for each soil layer are input data for BBGCMuSo. Based on soil texture, other soil properties (characteristic points of SWC, B, BD) can be estimated internally by the model using pedotransfer functions (Fodor and Rajkai, 2011). The default values are listed in Table 2, which can be adjusted by the user within their plausible ranges.

As in the original Biome-BGC, the PSI at saturation is the function of soil texture in BBGCMuSo:

$$\mathrm{PSI_{sat}} = -\{\exp[(1.54 - 0.0095 \cdot \mathrm{SAND} + 0.0063 \cdot \mathrm{SILT}) \cdot \ln(10)] \cdot 9.8 \cdot 10^{-5}\}, \quad (1)$$

where SAND and SILT are the sand and silt percent fractions of the soil, respectively. In BBGCMuSo, PSI for unsaturated soils is calculated from SWC using the saturation value of SWC ($\mathrm{SWC_{sat}}$) and the B parameter:

$$\mathrm{PSI} = \exp\left(\frac{\mathrm{SWC_{sat}}}{\mathrm{SWC}} \cdot \ln(B)\right) \cdot \mathrm{PSI_{sat}}. \quad (2)$$

Pond water and hygroscopic water

In the case of intensive rainfall events, when not all of the precipitation can infiltrate, pond water is formulated at the surface. Water from the pond can infiltrate the soil after the water content of the top soil layer decreases below saturation. Evaporation of the pond water is assumed to be equal to potential soil evaporation.

SWC (as well as C and N content) is not allowed to become negative. The theoretical lower limit of SWC is the hygroscopic water, i.e., the water content of air-dried soil. Therefore, in the case of large calculated evapotranspiration (calculated based on the Penman–Monteith equation as driven by meteorological data) and dry soil, the soil water

Table 2. Default values of parameters in BBGCMuSo for different soil types. Soil types are identified based on the user-defined sand, silt, and clay fraction of the soil layers based on the soil triangle method.

	Sand	Loamy sand	Sandy loam	Sandy clay	Sandy clay loam	Loam	Silt loam	Silt	Silty clay loam	Clay loam	Silty clay	Clay
B	3.45	10.45	9.22	5.26	4.02	50	7.71	7.63	6.12	5.39	4.11	12.46
SWC_{sat}	0.4	0.52	0.515	0.44	0.49	0.51	0.505	0.5	0.46	0.48	0.42	0.525
SWC_{fc}	0.155	0.445	0.435	0.25	0.38	0.42	0.405	0.39	0.31	0.36	0.19	0.46
SWC_{wp}	0.03	0.275	0.26	0.09	0.19	0.24	0.22	0.205	0.13	0.17	0.05	0.29
BD	1.60	1.4	1.42	1.56	1.5	1.44	1.46	1.48	1.54	1.52	1.58	1.38
RCN	50	70	68	54	56	64	66	62	58	60	52	72

B (dimensionless): Clapp–Hornberger parameter; SWC_{sat}, SWC_{fc}, SWC_{wp} ($m^3\,m^{-3}$): SWCs at saturation, at the field capacity and at the wilting point, respectively; BD ($g\,cm^{-3}$): bulk density; RCN (dimensionless): runoff curve number.

pool of the top layer can be depleted (approaching hygroscopic water content). In this case, evaporation and transpiration fluxes are limited in BBGCMuSo. Hygroscopic water content is also the lower limit in decomposition calculations (see below).

Runoff

Our runoff simulation method is semi-empirical and uses the precipitation amount and the Soil Conservation Service (SCS) runoff curve number (Williams, 1991). If the precipitation is greater than a critical amount which depends on the water content of the topsoil, a fixed part of the precipitation is lost due to runoff and the rest infiltrates the soil. The runoff curve number can be set by the user or can be estimated by the model (Table 2).

Percolation and diffusion

In BBGCMuSo, two calculation methods of vertical soil water movement are implemented. The first method is based on Richards' equation (Chen and Dudhia, 2001; Balsamo et al., 2009). A detailed description and equations for this method can be found in Hidy et al. (2012). The second method is the so-called "tipping bucket method" (Ritchie, 1998) which is based on semi-empirical estimation of percolation and diffusion fluxes and has a long tradition in crop modeling.

In the case of the first method, hydraulic conductivity and hydraulic diffusivity are used in diffusion and percolation calculations. These variables change rapidly and significantly upon changes in SWC. As we already mentioned, for the calculation of the main processes, a daily time step is used. For the calculation of the soil hydrological processes, finer temporal resolution was implemented in the case of the first calculation method (in the case of the tipping bucket method, a daily time step is used).

In BBGCMuSo, the time step (TS; seconds) of the soil water module integration is dynamically changed. In contrast to the modified Biome-BGC (Hidy et al., 2012), the TS is based on the theoretical maximum of soil water flux instead of the amount of precipitation.

As a first step, we calculate water flux data for a short, 1 s TS for all soil layers based on their actual SWC. The most important problem here is the selection of the optimal TS: TS values that are too small result in a slow model run, while TS values that are too large will lead to overestimation of water fluxes. The TS is estimated based on the magnitude of the maximal soil moisture content change in 1 s (ΔSWC_{max}; $m^3\,m^{-3}\,s^{-1}$). Equations (3)–(4) describes the calculation of TS:

$$TS = 10^{EXPON}, \tag{3}$$

where

$$\begin{aligned} EXPON &= abs\,[LV + (DL + 3)] \text{ if } DL + LV < 0 \\ EXPON &= 0 \qquad\qquad\quad \text{if } DL + LV \geq 0 \end{aligned}. \tag{4}$$

LV is the rounded local value of the maximal soil moisture content change, and DL is the discretization level, which can be 0, 1, or 2 (low, medium, or high discretization level which can be set by the user).

Therefore, if the magnitude of ΔSWC_{max} is $10^{-3}\,m^3\,m^{-3}\,s^{-1}$ (e.g., SWC increases from 0.400 to $0.401\,m^3\,m^{-3}$ in 1 s), then LV is -3, so TS is $10^0 = 1$ s (if DL = 0). The 1 s TS is necessary if ΔSWC_{max} is above $10^{-1}\,m^3\,m^{-3}\,s^{-1}$. Using daily TS proved to be adequate when ΔSWC_{max} was below $10^{-8}\,m^3\,m^{-3}\,s^{-1}$.

After calculating the first TS ($TS_{step1} = 1$ s), water fluxes are determined by using the precalculated time steps, and the SWC of the layers are updated accordingly. In the next n steps the calculations are repeated until reaching a threshold (86 400, the number of the seconds in a day). This method helps to avoid the overestimation of the water fluxes while also decreasing the computation time of the model.

4.1.3 Groundwater

Poorly drained forests (e.g., in boreal regions or in lowland areas) are special ecosystems where groundwater and flooding play an important role in soil hydrology and plant growth (Bond-Lamberty et al., 2007a; Pietsch et al., 2003). In order to enable groundwater effects (vertically varying soil water saturation), we implemented an option in BBGCMuSo to

supply external information about the depth of the water table. Groundwater depth is controlled by prescribing the depth of saturated zone (groundwater) within the soil. We note that the groundwater implementations by Pietsch et al. (2003) and by Bond-Lamberty et al. (2007a) are different from our approach as they calculate water table depth internally with the modified Biome-BGC. During the spinup phase of the simulation, the model can only use daily average data for one typical simulation year (i.e., multiannual mean water table depth). During the normal phase, the model can read daily groundwater information defined externally.

The handling of the externally supplied, near-surface groundwater information is done as follows. If the upward-moving water table reaches the bottom border of a simulated soil layer, part of the given layer becomes "quasi-saturated" (99 % of the saturation value), and thus the average soil moisture content of the given layer increases. If the water table reaches the upper border of the given soil layer, then the given layer becomes quasi-saturated. The quasi-saturation state allows for the downward flow of water through a saturation soil layer, particularly through the last layer. This approach was necessary because of the discrete size of soil layers and the fact that the input groundwater level data constitute a net groundwater level. Namely, groundwater level is partly affected by lateral groundwater flows (which are unknown) and corresponding changes in hydraulic pressure that can push the water up; it is also partly affected by draining of the upper soil layers. While soil is draining, it is possible that the groundwater level remains unchanged, or that its level decreases slower because the drained water from the upper layer replaces the water that leaves the system (i.e., drains to below 10 m, which is the bottom of the last soil layer). With implementation of quasi-saturation state, we allowed for the water to flow through saturated layers, in particular through the bottom one. Otherwise, the water could become "trapped" because the model routine could not allow downward movement of water from an upper soil layer to a lower layer that is already saturated (because that layer would have already been "full").

Groundwater level affects soil water content and in turn affects stomatal conductance and soil organic matter decomposition (see below).

4.1.4 Root distribution

Water becomes available to the plant through water uptake by the roots. The maximum depth of the rooting zone is a user-defined parameter in the model. For herbaceous vegetation, the temporally changing depth of the root is simulated based on an empirical, sigmoid function (Campbell and Diaz, 1988). In forests, fine root growth is assumed to occur in the entire root zone and rooting depth does not change with time. This latter logic is used due to the presence of coarse roots in forests which are assumed to change depth slowly (in juvenile forests, this approach might be problematic).

In order to weight the relative importance of the soil layers (i.e., to distribute total transpiration or root respiration among soil layers), it is necessary to calculate the distribution of roots in the soil layers. The proportion of the total root mass in the given layer (R_{layer}) is calculated based on empirical exponential root profile approximation after Jarvis (1989):

$$R_{\mathrm{layer}} = f \cdot \left(\frac{\Delta z_{\mathrm{layer}}}{z_{\mathrm{r}}}\right) \cdot \exp\left[-f \cdot \left(\frac{z_{\mathrm{layer}}}{z_{\mathrm{r}}}\right)\right]. \quad (5)$$

In Eq. (5), f is an empirical root distribution parameter (its proposed value is 3.67 after Jarvis, 1989), $\Delta z_{\mathrm{layer}}$ and z_{layer} are the thickness and the midpoint of the given soil layer, respectively, and z_{r} is the actual rooting depth.

Rooting depth and root distribution are taken into account by all ecophysiological processes which are affected by soil moisture content (transpiration), soil carbon content (maintenance respiration), and soil N content (decomposition).

4.1.5 Nitrogen budget

In previous model versions, uniform distribution of mineral N was assumed within the soil profile. In BBGCMuSo, we hypothesize that varying amounts of mineralized N are available within the different soil layers and are available for root uptake and other losses. The change of soil mineral N content is calculated layer by layer in each day. In the root zone (i.e., within soil layers containing roots), the changes of mineralized N content are caused by soil processes (decomposition, microbial immobilization, denitrification), plant uptake, leaching, atmospheric deposition, and biological N fixation. The produced/consumed mineralized N (calculated by decomposition and daily allocation functions) is distributed within the layers depending on their soil mineral N content. Mineralized N from atmospheric N deposition (Ndep) increases the N content of the first (0–10 cm) soil layer. Biological N fixation is divided between root zone layers as a function of the root fraction in the given layer. In soil layers without roots, N content is affected by transport (e.g., leaching) only. Leaching is calculated based on empirical function using the proportion of soluble N that is subject to mobilization (an adjustable ecophysiological parameter in the model), mineral N content and the water fluxes (percolation and diffusion) of the different soil layers.

There is an additional mechanism for N loss within the soil. According to the model logic (Thornton and Rosenbloom, 2005) if there is excess mineral nitrogen in the soil following microbial immobilization and plant N uptake, it is subject to volatilization and denitrification as a constant proportion of the excess mineral nitrogen pool for a given day. In the original Biome-BGC (v4.1.1), this proportion was defined by a fixed parameter within the model code. In Biome-BGC v4.2, two parameters were introduced that control bulk denitrification: one for the wet case and one for the dry case (the wet case is defined as when SWC is greater than 95 % of saturation). In BBGCMuSo, we implemented the Biome-

BGC v4.2 logic, which means that these values can be adjusted as part of the ecophysiological model parameterization.

4.1.6 Soil moisture stress index

Stomatal closure occurs due to low relative atmospheric moisture content (high VPD), and insufficient soil moisture (drought stress; Damour et al., 2010) but also due to anoxic conditions (e.g., presence of elevated groundwater or high soil moisture content during and after large precipitation events; Bond-Lamberty et al., 2007a). The original Biome-BGC had a relatively simple soil moisture stress function which was not adjustable and was unable to consider anoxic conditions.

In order to create a generalized model logic for BBGC-MuSo, the soil moisture limitation calculation was improved, and the use of the stress function on stomatal conductance (and consequently transpiration and senescence) calculations was extended, taking into account both types of limitations mentioned above (limit1: drought, limit2: anoxic condition close to soil saturation). The start and end of the water stress period are determined by comparing actual and predefined, characteristic points of SWC and calculating a novel soil moisture stress index (SMSI; dimensionless). Characteristic points of soil water status can be defined using relative SWC (relative SWC to field capacity in the case of limit1 and to saturation in the case of limit2) or soil water potential (see Sect. 3.4 of Hidy et al., 2015).

SMSI is the function of normalized soil water content (NSWC) (in contrast to original model, where SMSI was the function of soil water potential). NSWC is defined by the following equation:

$$\begin{aligned} \mathrm{NSWC} &= \frac{\mathrm{SWC}-\mathrm{SWC_{wp}}}{\mathrm{SWC_{sat}}-\mathrm{SWC_{wp}}}, \text{if } \mathrm{SWC_{wp}} < \mathrm{SWC} \\ \mathrm{NSWC} &= 0 \qquad\quad , \text{if } \mathrm{SWC_{wp}} \geq \mathrm{SWC} \end{aligned} \quad , \qquad (6)$$

where SWC is the soil water content of the given soil layer ($m^3\ m^{-3}$), SWC_{wp} and SWC_{sat} are the wilting point and the saturation value of soil water content, respectively. Parameters can either be set by the user or calculated by the model internally (see Table 2).

The NSWC and the soil water potential as function of SWC are presented in Fig. 1 for three different soil types: sand soil (sand: 90 %, silt: 5 %), sandy clay loam (sand: 50 %, silt: 20 %), and clay soil (sand: 8 %, silt: 45 %).

According to our definition, SMSI is a function of NSWC and can vary between 0 (maximum stress) and 1 (minimum stress).

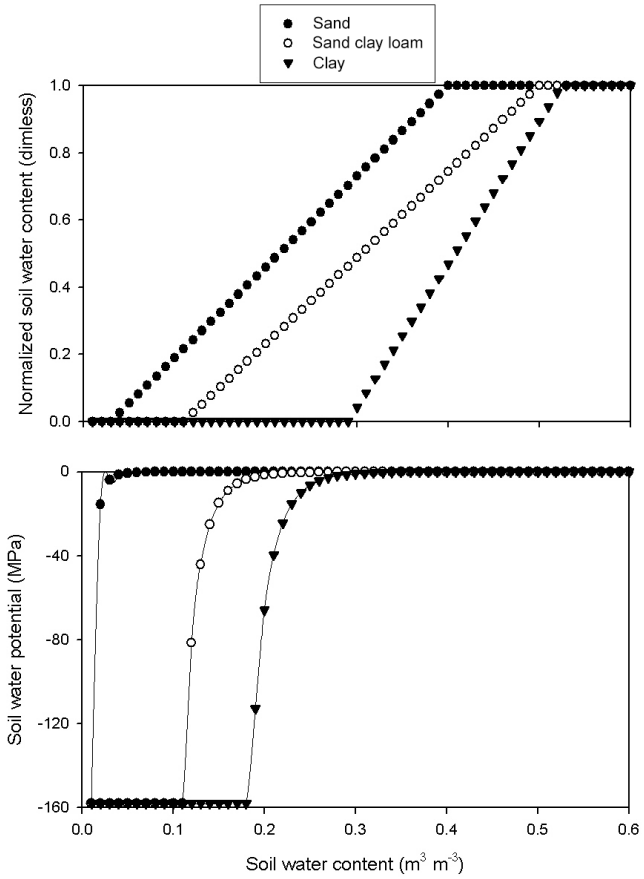

Figure 1. Dependence of normalized soil water content (upper part) and soil water potential (lower part) on soil water content in the case of three different soil types. Dimless indicates dimensionless measurements.

The general form of SMSI is defined by the following equations:

$$\begin{aligned} \mathrm{SMSI} &= \frac{\mathrm{NSWC}}{\mathrm{NSWC_{crit1}}}, \quad \text{if } \mathrm{NSWC} < \mathrm{NSWC_{crit1}} \\ \mathrm{SMSI} &= 1, \qquad \text{if } \mathrm{NSWC_{crit1}} < \mathrm{NSWC} \leq \mathrm{NSWC_{crit2}}, \\ \mathrm{SMSI} &= \frac{1-\mathrm{NSWC}}{1-\mathrm{NSWC_{crit2}}}, \text{if } \mathrm{NSWC_{crit2}} < \mathrm{NSWC} \end{aligned} \qquad (7)$$

where $NSWC_{crit1}$ and $NSWC_{crit2}$ ($NSWC_{crit1} < NSWC_{crit2}$) are the characteristic points of the normalized soil water curve, calculated from the soil water potential values or relative soil water content defined by ecophysiological parameters. Conversion from relative values to NSWC is made within the model. Characteristic point $NSWC_{crit1}$ is used to control drought-related limitation, while $NSWC_{crit2}$ is used to control excess-water-related limitation (e.g., anoxic-soil-related stomatal closure).

The shape of the soil stress function in the original model (based on soil water potential) and in BBGCMuSo (based on NSWC) are presented in Fig. 2.

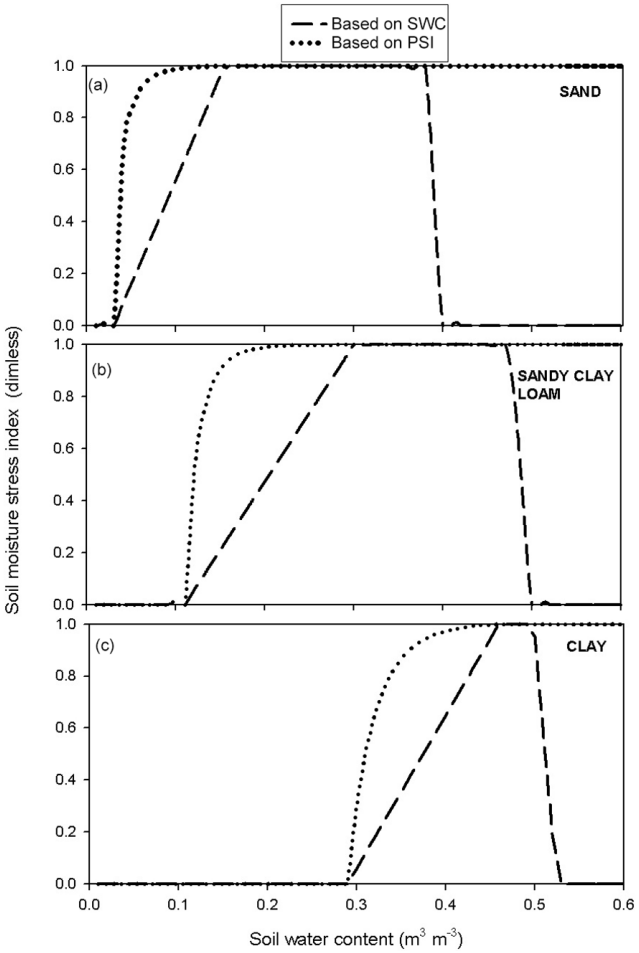

Figure 2. Dependence of the soil moisture stress index on soil water content for three different soil types: sand **(a)**, sandy clay soil **(b)**, and clay **(c)**. Soil stress index based on soil water potential (dotted lines) is used by the original model, while soil stress index based on normalized soil water content is used by BBGCMuSo (dashed lines).

The value of the SMSI is zero in the case of full soil water stress (below the wilting point). It starts to increase at the wilting point (which depends on soil type; Table 1) and reaches its maximum (1) at the SWC where water stress ends. This latter characteristic value can be set by the user. In this example (Fig. 2), field capacity was used as the characteristic value. The new feature of the BBGCMuSo is that beyond the optimal soil moisture content range, the soil stress can decrease again (i.e., increasing stress) due to saturation. This second characteristic value (limit2) can also be set by a model parameter. In the example of Fig. 2, 95 % of the saturation value was used as the second characteristic value.

Though soil water status is calculated layer by layer, the model requires a single soil moisture stress function to calculate stomatal conductance. To satisfy this need, an average stress function for the total root zone is necessary, which is the average of the layer factors weighted by root fraction in each layer.

Besides stomatal conductance, SMSI is used in the transpiration calculation in the multilayer soil. Instead of the averaged soil water status of the whole soil column (as in the original Biome-BGC), in BBGCMuSo, the transpiration flux is calculated layer by layer. The transpiration flux of the ecosystem is assumed to be equal to the total root water uptake on a given day (TRP_{sum}). The transpiration calculation is based on the Penman–Monteith equation using stomatal conductance (this feature is the same as in the original Biome-BGC method). The transpiration fluxes are divided between layers (TRP_{layer}) according to the soil moisture limitation of the given layer ($SMSI_{layer}$) and the root fraction in the given layer (R_{layer} in Eq. 5):

$$TRP_{layer} = TRP_{sum} \cdot \frac{SMSI_{layer} \cdot R_{layer}}{SMSI_{sum}}, \quad (8)$$

where $SMSI_{sum}$ is the sum of the $SMSI_{layer}$ values in the root zone.

According to the modifications, if the soil moisture limitation is full ($SMSI = 0$), no transpiration can occur.

4.1.7 Senescence calculation

The original Biome-BGC ignores plant wilting and associated senescence (where the latter is an irreversible process) caused by prolonged drought. In order to solve this problem, a new module was implemented to simulate the ecophysiological effect of drought stress on plant mortality. A senescence simulation has already been implemented in developed Biome-BGC (Hidy et al., 2012) and it was further improved in BBGCMuSo following a different approach. In BBGCMuSo, if the plant-available SWC decreases below a critical value, the new module starts to calculate the number of the days under drought stress. Due to low SWC during a prolonged drought period, aboveground and belowground plant material senescence is occurring (actual, transfer, and storage C and N pools) and the wilted biomass is translocated into the litter pool.

A so-called "soil stress effect" (SSE_{total}) is defined to calculate the amount of plant material that wilts due to cell death in 1 day due to drought stress. The SSE_{total} quantifies the severity of the drought for a given day. Severity of drought is a function of the number of days since soil moisture stress is present (NDWS). Soil water stress is assumed if the averaged SMSI of the root zone is less than a critical value (which is an adjustable ecophysiological parameter in the model). It is assumed that after a longer time period with soil moisture stress, the senescence is complete and no living non-woody plant material remains. This longer time period is quantified by an ecophysiological parameter, which is the "critical number of stress days after which senescence mortality is complete".

The SSE_{total} varies between 0 (no stress) and 1 (total stress). According to the BBGCMuSo logic, the SSE_{total} is the function of SMSI, NDWS, $NDWS_{crit}$, and $SMSI_{crit}$:

$$\begin{aligned} SSE_{total} &= SSE_{SMSI} \cdot SSE_{NDWS} \\ SSE_{SMSI} &= \left(1 - \frac{SMSI}{SMSI_{crit}}\right); \text{ if } SMSI < SMSI_{crit} \\ SSE_{SMSI} &= 0 \quad ; \text{ if } SMSI \geq SMSI_{crit} \\ SSE_{NDWS} &= \frac{NDWS}{NDWS_{crit}} \; ; \text{ if } NDWS < NDWS_{crit} \\ SSE_{NDWS} &= 1 \quad ; \text{ if } NDWS \geq NDWS_{crit} \end{aligned} \quad . \tag{9}$$

The SEE_{total} is used to calculate the actual value of non-woody aboveground and belowground mortality defined by SMCA and SMCB, respectively. SMCA defines the fraction of living C and N that dies in 1 day within leaves and herbaceous stems. SMCB does the same for fine roots. SMCA and SMCB are calculated using two additional ecophysiological parameters: minimum mortality coefficient (minSMC) of non-woody aboveground (A) and belowground (B) plant material senescence (minSMCA and minSMCB, respectively):

$$\begin{aligned} SMCA &= \text{minSMCA} + (1 - \text{minSMCA}) \cdot SSE_{total} \\ SMCB &= \text{minSMCB} + (1 - \text{minSMCB}) \cdot SSE_{total} \end{aligned} \quad . \tag{10}$$

Parameters minSMCA and minSMCB can vary between 0 and 1. In the case of 0, no senescence occurs. In the case of 1, all living C and N will die within 1 day after the occurrence of drought stress. In this sense, SMCA and SMCB can vary between their minimum value (minSMCA and minSMCB, respectively, if SSE_{total} is zero) and 1 (if SSE_{total} is 1). This latter case occurs when $NDWS > NDWS_{crit}$ and $SMSI = 1$.

SMCA is used to calculate the amount of non-woody aboveground plant material (leaves and soft stem) transferred to the standing dead biomass pool (STDB; kgC m^{-2}) due to soil moisture stress-related mortality on a given day. Note that STDB is a temporary pool from which C and N contents transfer to the litter pool gradually; the concept of STDB is a novel feature in the model. In the case of belowground mortality, it defines the amount of fine root that goes to the litter pool directly. The actual senescence ratio is calculated as SMCA (and SMCB) multiplied with the actual living C and N pool.

Figure 3 demonstrates the senescence calculation with an example. The figure shows the connections between the change of SWC, normalized soil water content, SMSI, different types of soil stress effects (SSE_{SMSI}, SSE_{NDWS}, SSE_{total}), and senescence mortality coefficient as function of number of days since water stress is present. The figure shows a theoretical situation in which SWC decreases from field capacity to hygroscopic water within 30 days. The calculation refers to a sandy soil ($SWC_{sat} = 0.44\ m^3\ m^{-3}$, $SWC_{fc} = 0.25\ m^3\ m^{-3}$, $SWC_{wp} = 0.09\ m^3\ m^{-3}$; SWC_{fc} refers to SWC at field capacity). In this example, we assumed that $relSWC_{crit1}$ is 1.0 (field capacity) and $relSWC_{crit2} = 0.9$ (10 % below saturation), the critical number of stress days after which senescence mortality is complete ($NDWS_{crit}$) is 30 and the critical soil moisture stress index ($SMSI_{crit}$) is 0.3.

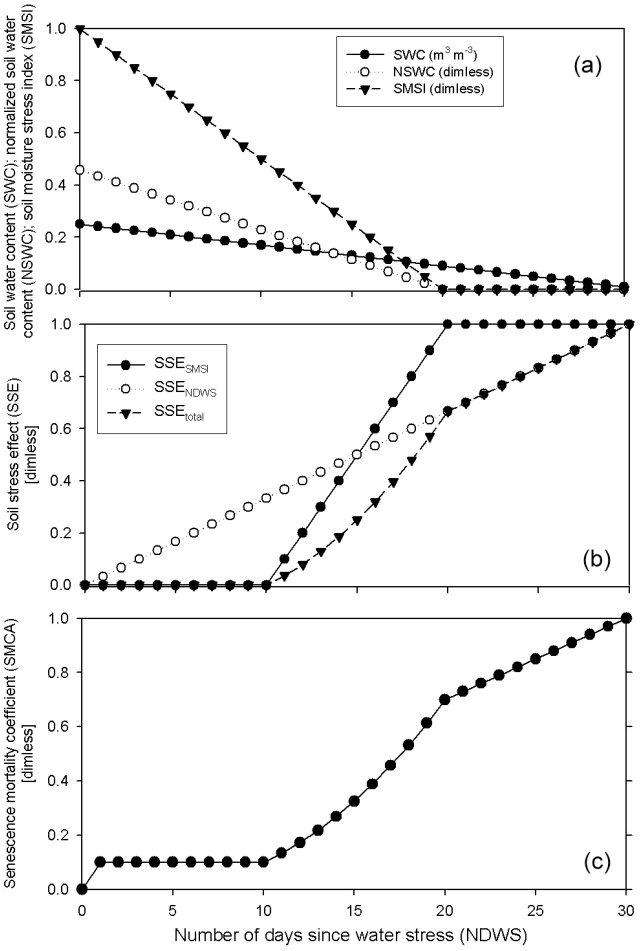

Figure 3. Demonstration of the senescence calculation with an example. **(a)** Soil water content (SWC; black dots), normalized soil water content (NSWC; white dots) and soil moisture stress index (SMSI; black triangles) during 30 days of a hypothetical drought event. **(b)** Soil stress effect based on soil moisture stress index (SSE_{SMSI}; black dots), soil stress effect based on number of days since water stress (SSE_{NDWS}) and total soil stress effect (SSE_{total}). **(c)** Aboveground senescence mortality coefficient (SMCA).

4.1.8 Decomposition and respiration processes

Within Biome-BGC, decomposition processes of litter and soil organic matter are influenced by soil temperature, soil water status, soil and litter C and N content, while root maintenance respiration is affected by soil temperature and root C and N content. In BBGCMuSo, the soil moisture and temperature limitation effects are calculated layer by layer based on the SWC and soil temperature of the given soil layer (instead of the averaged soil water status or soil temperature of the whole soil column as in the original model). The C and

N contents are also calculated layer by layer from the total C and N content of the soil column weighted by the proportion of the total root mass in the given layer.

The maintenance root respiration flux is calculated based on the following equation:

$$\mathrm{MR(root)} = \sum_{\mathrm{layer}=1}^{n_\mathrm{r}} \left(N_\mathrm{root} \cdot R_\mathrm{layer} \cdot \mathrm{mrpern} \cdot Q_{10}^{\frac{T(\mathrm{soil})_\mathrm{layer}-20}{10}} \right), \quad (11)$$

where n_r is the number of the soil layers which contain root, N_root is the total N content of the soil, R_layer is the proportion of the total root mass in the given layer, mrpern is an adjustable ecophysiological parameter (maintenance respiration per kg of tissue N), Q_{10} is the fractional change in respiration with a 10 °C temperature change, and $T(\mathrm{soil})_\mathrm{layer}$ is the soil temperature of the given layer.

There are eight types of non-N limited fluxes between litter and soil compartments. These fluxes are the function of soil and litter C or N content, soil moisture, and soil temperature stress functions. The most important innovation is that total decomposition fluxes are calculated as the sum of partial fluxes regarding to the given layer similarly to respiration flux. The soil temperature function is the same as in the original Biome-BGC. The soil moisture stress function is a linear function of SWC in contrast to a logarithmic function of soil water potential in the original Biome-BGC. A major development here is that, besides drought effect, anoxic stress is also taken into account because anoxic conditions caused by saturation can affect decomposition of soil organic matter (and thus N mineralization; Bond-Lamberty et al., 2007a). The shape of the modified stress index ($\mathrm{SMSI_{decomp}}$) is similar to the one presented in Bond-Lamberty et al. (2007a).

BBGCMuSo uses the following stress index (with values between 0 and 1) to control decomposition in response to changing SWC in a given layer:

$$\begin{aligned} \mathrm{SMSI_{decomp}} &= \frac{\mathrm{SWC} - \mathrm{SWC_{hyg}}}{\mathrm{SWC_{opt}} - \mathrm{SWC_{hyg}}}, \text{if } \mathrm{SWC} \le \mathrm{SWC_{opt}} \\ \mathrm{SMSI_{decomp}} &= \frac{\mathrm{SWC_{sat}} - \mathrm{SWC}}{\mathrm{SWC_{sat}} - \mathrm{SWC_{opt}}}, \text{if } \mathrm{SWC_{opt}} < \mathrm{SWC} \end{aligned}, \quad (12)$$

where SWC, $\mathrm{SWC_{hyg}}$, and $\mathrm{SWC_{sat}}$ is the actual soil water content, hygroscopic water, and the saturation values of the given soil layer, respectively. $\mathrm{SWC_{opt}}$ is calculated from the relative SWC for soil moisture limitation, which is a user-supplied ecophysiological input parameter. The limitation function of decomposition in the original Biome-BGC (based on PSI) and in BBGCMuSo (based on SWC) are presented in Fig. 4.

In the case of the original model, soil stress index starts to increase at −10 MPa (this value is fixed in the model) and reaches its maximum at saturation. In the case of BBGCMuSo, soil stress index starts to increase at hygroscopic water and reaches its maximum at optimal SWC (which is equal to the $\mathrm{NSWC_{crit2}}$ from Eq. 7). The new feature of BBGCMuSo is that after the optimal soil moisture content, soil stress index can decrease due to saturation soil stress (anoxic soil).

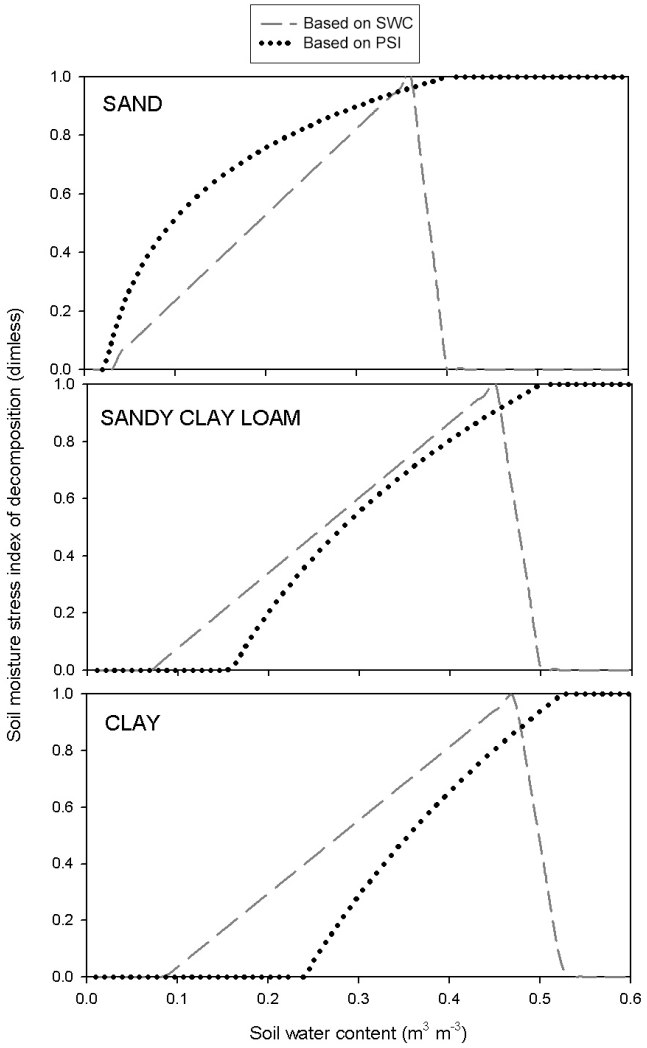

Figure 4. Soil moisture stress index used by decomposition for three different soil types: sand **(a)**, sandy clay soil **(b)**, and clay **(c)**. Soil stress index based on soil water potential (dotted lines) is used by the original model, while soil stress index based on soil water content is used by BBGCMuSo (dashed grey lines).

4.2 Management modules

The original Biome-BGC was developed to simulate natural ecosystems with very limited options to disturbance or human intervention (fire effect is an exception). Lack of management options limited the applicability of Biome-BGC in croplands and grasslands, but also in managed forests.

One major feature of BBGCMuSo is the implementation of several management options. For grasslands, grazing and

mowing modules were already published as part of the developed Biome-BGC (Hidy et al., 2012).

Since the release of the developed Biome-BGC, we improved the model's ability to simulate management. In BBGCMuSo, the user can define seven different events for each management activity, and additionally annually varying management activities can be defined. Further technical information about using annually varying management activities is detailed in Sect. 3.2. of the user guide (Hidy et al., 2015). Additionally, new management modules were implemented and the existing modules were further developed and extended. The detailed description of mowing and grazing can be found in Hidy et al. (2012).

4.2.1 Harvest

In arable crops, the effect of harvest is similar to the effect of mowing in grasslands, but the fate of the cut-down fraction of aboveground biomass is different. We assume that after harvest, snags (stubble) remain on the field as part of the accumulated biomass, and part of the plant residue may be left on the field (in the form of litter typically to improve soil quality). Yield is always transported away from the field, while stem and leaves may be transported away (and utilized, e.g., as animal bedding) or may be left at the site. The ratio of harvested aboveground biomass that is taken away from the field has to be defined as an input.

If residue is left at the site after harvest, the cut-down plant material first goes into a temporary pool that gradually enters the litter pool. The turnover rate of mown/harvested biomass to litter can be set as an ecophysiological parameter. Although harvest is not possible outside the growing season, this temporary pool can contain plant material also in the dormant period (depending on the amount of the cut-down material and the turnover rate of the pool). The plant material turning into litter compartment is divided between the different types of litter pools according to the parameterization (based on unstable, cellulose, and lignin fractions). The water stored in the canopy of the cut-down fraction is assumed to be evaporated.

4.2.2 Ploughing

As a management practice, ploughing may be carried out in preparation for sowing or following harvest. Three types of ploughing can be defined in BBGCMuSo: shallow, medium, and deep (first; first and second; first, second, and third soil layers are affected, respectively). Ploughing affects the predefined soil texture, as it homogenizes the soil (in terms of texture, temperature, and moisture content) for the depth of the ploughing. We assume that due to the plough the snag or stubble turns into a temporary ploughing pool on the same day. A fixed proportion of the temporary ploughing pool (an ecophysiological parameter) enters the litter pool on a given day after ploughing. The plant material turning into the litter compartment is divided between the different types of litter pools (labile, unshielded cellulose, shielded cellulose, and lignin).

A new feature of Biome-BGCMuSo is that aboveground and belowground (buried) litter is handled separately in order to support future applications of the model in cropland-related simulations (presence of crop residues at the surface affects runoff and soil evaporation). As a consequence of litterfall during the growing season and the result of harvest, litter accumulates at the surface. In the case of ploughing, the content of aboveground litter turns into the belowground litter pool. In this way, aboveground/belowground litter amount can be quantified.

4.2.3 Fertilization

The most important effect of fertilization in BBGCMuSo is the increase of mineralized soil nitrogen. We define an actual pool which contains the amount of fertilizer's nitrogen content put out onto the ground on a given fertilizing day (actual pool of fertilizer; APF). A fixed proportion of the fertilizer enters the top soil layer on a given day after fertilizing. It is not the entire fraction that enters the soil because a given proportion is leached (this is determined by the efficiency of utilization that can be set as an input parameter). Nitrate content of the fertilizer (that has to be set by the user) can be taken up by the plant directly; therefore, we assume that it goes into the soil mineral N pool. Ammonium content of the fertilizer (that also has to be set by the user) has to be nitrified before being taken up by plants; therefore, it turns into the litter nitrogen pool. C content of fertilizer turns into the litter C pool. As a result, APF decreases day by day after fertilizing until it becomes empty, which means that the effect of the fertilization ends (in terms of N input to the ecosystem).

4.2.4 Planting

In BBGCMuSo, transfer pools are defined to contain plant material as a germ (or bud or nonstructural carbohydrate) in the dormant season from which C and N get to the normal pools (leaf, stem, and root) in the beginning of the subsequent growing season. In order to simulate the effect of sowing, we assume that the plant material which is in the planted seed goes into the transfer pools, thus increasing its content. Allocation of leaf, stem, and root from seed is calculated based on allocation parameters in the ecophysiological input data. We assume that a given part of the seed is destroyed before sprouting (this can be adjusted by the user).

4.2.5 Thinning

Forest thinning is a new management option in BBGCMuSo. We assume that based on a thinning rate (the proportion of the removed tree volume), the decrease of leaf, stem, and root biomass pools can be determined. After thinning, the cut-down fraction of the aboveground biomass can be taken away

or can be left at the site. The rate of transported stem and/or leaf biomass can be set by the user. The transported plant material is excluded from further calculations. The plant material translocated into coarse woody debris (CWD) or litter compartments are divided between the different types of litter pools according to parameterization (coarse root and stem biomass go into the CWD pool; if harvested stem biomass is taken away from the site, only coarse root biomass goes to CWD). Note that storage and transfer pools of woody harvested material are translocated into the litter pool.

The handling of the cut-down, non-removed pools differs for stem, root, and leaf biomass. Stem biomass (live and deadwood; see Thornton, 2000 for definition of deadwood in the case of Biome-BGC) is immediately translocated into CWD without any delay. However, for stump and leaf biomass implementation, an intermediate turnover process was necessary to avoid C and N balance errors caused by sudden changes between specific pools. The parameter "turnover rate of cut-down, non-removed, non-woody biomass to litter" (ecophysiological input parameter) controls the fate of (previously living) leaves on cut-down trees, and it also controls the turnover rate of dead coarse root (stump) into CWD.

4.2.6 Irrigation

In the case of the novel irrigation implementation, we assume that the sprinkled water reaches the plant and the soil similarly to precipitation. Depending on the amount of the water reaching the soil (canopy water interception is also considered) and the soil type, the water can flow away by surface runoff process while the rest infiltrates the top soil layer. Irrigation amount and timing can be set by the user.

4.2.7 Management-related plant mortality

In the case of mowing, grazing, harvest, and thinning, the main effect of the management activity is the decrease of the aboveground plant material. It can be hypothesized that due to the disturbance-related mortality of the aboveground plant material, the belowground living plant material also decreases but at a lower (and hardly measurable) rate. Therefore, in BBGCMuSo we included an option to simulate the decrease of the belowground plant material due to management that affects aboveground biomass. The rate of the belowground decrease to the mortality rate of the aboveground plant material can be set by the user. As an example, if this parameter is set to 0.1, the mortality rate of the belowground plant material is 10 % of the mortality of the aboveground material on a given management day. Aboveground material refers to actual pool of leaf, stem, and fruit biomass while belowground material refers to actual pool of root biomass and all the storage-transfer pools.

4.3 Other plant-related model processes

The original Biome-BGC had a number of static features that limited its applicability in some simulations. In Biome-BGC, we added new features that can support model applications in a wider context, e.g., in climate-change-related studies and modeling exercises comparing free air CO_2 enrichment (FACE) experiment data with simulations (Franks et al., 2013).

4.3.1 Phenology

To determine the start and end of the growing season, the phenological state simulated by the model can be used (White et al., 1999). We have enhanced the phenology module of the original Biome-BGC, keeping the original logic and providing the new method as an alternative. We developed the so-called heat sum growing season index (HSGSI; Hidy et al., 2012), which is the extension of the GSI index proposed by Jolly et al. (2005).

In the original, as well as in the modified Biome-BGC model versions, snow cover did not affect the start of the vegetation period and photosynthesis. We implemented a new, dual snow cover limitation method in BBGCMuSo. First, the growing season can only start if the snowpack is less than a critical amount (given as millimeters of water content stored in the snowpack). Second, the same critical value can also limit photosynthesis during the growing season (no C uptake is possible above the critical snow cover; we simply assume that in the case of low vegetation, no radiation reaches the surface if snow depth is above a predefined threshold). The snow cover estimation is based on precipitation, mean temperature and incoming shortwave radiation (original model logic is used here). The critical amount of snow can be defined by the user.

4.3.2 Genetically programmed leaf senescence

Besides drought-stress-related leaf senescence, an optional secondary leaf senescence algorithm was implemented in BBGCMuSo. For certain crops (e.g., maize and wheat), leaf senescence is the genetically programmed final stage of leaf development, as it is related to the age of the plant tissue in leaves. In crop models, this process is traditionally determined based on the growing degree-day (GDD) sum. GDD sum is a measure of heat accumulation to predict plant development stages such as flowering as well as the beginning and end of grain filling. GDD is calculated using the cumulative difference between mean daily temperature and base temperature (the latter is an ecophysiological input parameter in BBGCMuSo). In the case of planting (i.e., in crop-related simulations), GDD is calculated from the day of planting. In other cases, GDD is calculated from the beginning of the year. After reaching the predefined GDD threshold, leaf mortality rates are calculated based on a mortality coefficient of

genetically programmed leaf senescence (ecophysiological input parameter).

4.3.3 New plant pools: fruit and soft stem simulation

In order to enable C and N budget simulation of croplands and explicit yield estimation with BBGCMuSo, fruit simulation was implemented (which is grain in the case of croplands). Start of the fruit allocation is estimated based on GDD. After reaching a predefined GDD value (supplied by the user as an input parameter), fruit starts to grow (allocation is modified). Besides critical GDD, there are three additional ecophysiological parameters that have to be defined by the user that are related to allocation, C : N ratio of fruit, and labile and cellulose proportion of litter.

In order to support C and N budget simulation of non-woody biomass in BBGCMuSo, a soft stem simulation was implemented (soft stem is non-photosynthesizing, aboveground, non-woody biomass). Soft stem allocation is parallel to fine root and leaf allocation (and fruit allocation, if applicable). Four additional ecophysiological parameters are defined due to soft stem simulation. The primary purpose of our soft stem implementation is to decrease the overestimation of LAI in herbaceous vegetation calculations. In the original model structure, in the case of herbaceous vegetation, all aboveground plant material is allocated to leaves, which causes unrealistically high LAI in many cases. Soft stem allocation (a significant pool in, e.g., grasses and crops) enables more realistic leaf C and LAI values.

4.3.4 New C4 photosynthesis routine

In the original and modified Biome-BGC models, C_4 photosynthesis was expressed as a sub-version of C_3 photosynthesis. It was implemented in a way that only one parameter differed (photons absorbed by transmembrane protein complex per electron transported; mol mol^{-1}) for C_3 and C_4 plants (Collatz et al., 1991).

Based on the work of Di Vittorio et al. (2010), we implemented a new, enzyme-driven C_4 photosynthesis routine into the photosynthesis module. A new ecophysiological parameter (fraction of leaf N in PEP carboxylase) was defined in BBGCMuSo to support the C_4 routine. The ecophysiological parameter "fraction of leaf N in RuBisCO" still affects the process of C_4 photosynthesis (see Di Vittorio et al., 2010 for details).

4.3.5 Dynamic response and temperature acclimation of respiration

Due to the changing environmental conditions, photosynthesis and respiration acclimation and dynamic response of plants could affect the carbon exchange rates, but this mechanism is missing from many biogeochemical models (Smith and Dukes, 2012).

In order to implement acclimation and short-term temperature dependence of maintenance respiration in BBGCMuSo, the respiration module was modified in two steps. The maintenance respiration in Biome-BGC is based on a constant Q_{10} factor. In our approach, first the constant Q_{10} value was modified based on Tjoelker et al. (2001) who proposed an equation for the short-term temperature dependence of the Q_{10} factor (dynamic response), and showed how this relationship could improve the accuracy of the modeled respiration. We use the following equation:

$$Q_{10} = 3.22 - 0.046 \cdot T_{\text{air}}, \tag{13}$$

where T_{air} is the daily average air temperature (°C).

This modification results in a temperature optimum at which respiration peaks. The main influence of using a temperature-dependent Q_{10} value can be detected at high temperature values. In the case of a constant Q_{10}, overestimation of respiration can occur at higher temperatures (Lombardozzi et al., 2015).

The model of Tjoelker et al. (2001) is a more realistic method to calculate respiration but it does not take into account acclimation to the longer-term changes in thermal conditions.

Long-term responses of respiration rates to the temperature (i.e., acclimation) were implemented in the second step based on Atkin et al. (2008) who developed a method using the relationship between leaf respiration, leaf mass-to-area ratio, and leaf nitrogen content in 19 species of plants grown at four different temperatures. The proposed equation is the following:

$$R_A = R_T \cdot 10^{A \cdot (T_{10\ \text{days}} - T_{\text{ref}})}, \tag{14}$$

where R_T is the non-acclimated rate of respiration, T_{ref} is the reference temperature, $T_{10\,\text{days}}$ is the average daily temperature in the preceding 10 days, and A is a constant, which was set to 0.0079 based on Atkin et al. (2008). The acclimated and non-acclimated day and night leaf maintenance respiration functions are presented in Fig. 5.

Photosynthesis acclimation is in a test phase. It is simulated in a very simple way by modifying the relationship between V_{cmax} (maximum rate of carboxylation) and J_{max} (maximum electron transport rate) that was temperature independent in the original code. Temperature dependency is calculated based on average temperature for the previous 30 days (Knorr and Kattge, 2005). This simple photosynthesis method is not a complete representation of the acclimation of the photosynthetic machinery (Smith and Dukes, 2012) but a first step towards a more complete implementation. This feature can be enabled or disabled by the user.

4.3.6 LAI-dependent albedo

In order to improve the shortwave radiative flux estimation of BBGCMuSo, an LAI-dependent albedo estimation was

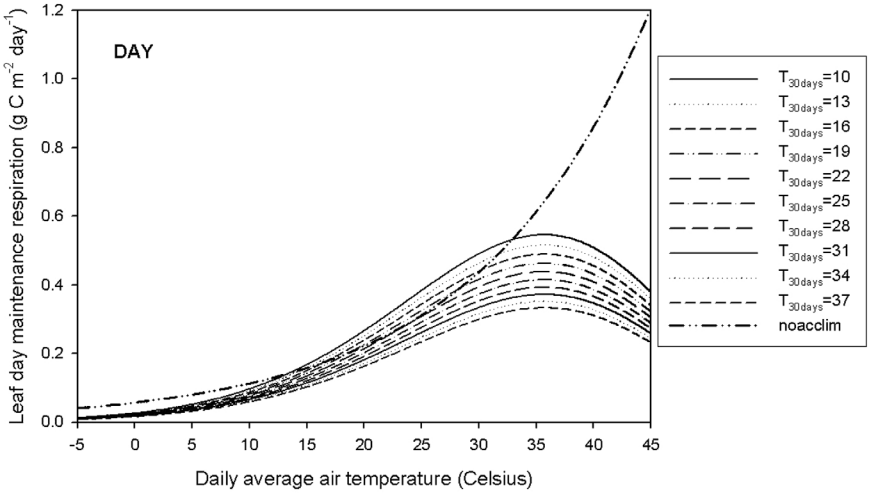

Figure 5. Acclimated and non-acclimated (noacclim) daytime maintenance respiration of leaf as a function of air temperature. Acclimated respiration values were calculated based on different average daily temperatures during the previous 30 days ($T_{30\,\mathrm{days}}$: 10, 13, 16, 19, 22, 25, 28, 31, 34, and 37 °C). In the case without acclimation, the respiration is independent of average daily temperature; therefore, only one line is presented (this refers to the original model logic).

implemented based on the method of Ritchie (1998). Actual albedo is calculated by the following equation:

$$\alpha_{\mathrm{act}} = \alpha_{\mathrm{crit}} - (\alpha_{\mathrm{crit}} - \alpha_{\mathrm{BS}}) \cdot \exp(-0.75 \cdot \mathrm{LAI}_{\mathrm{act}}), \quad (15)$$

where α_{crit} is an empirical estimate of the albedo maximum (0.23), α_{BS} is the albedo of the bare soil that has to be supplied by the user, and $\mathrm{LAI}_{\mathrm{act}}$ is the actual value of leaf area index as estimated by the model.

4.3.7 Stomatal conductance regulation

Although there are many alternative formulations for stomatal conductance calculation within biogeochemical models (e.g., Damour et al., 2010), there is no standard method in the scientific community. Many state-of-the-art ESMs use a variant of the Ball–Woodrow–Berry model (Ball et al., 1987), the Leuning (1995) method, and the Jarvis (1976) method. There is no proof that one method is significantly better than the others (Damour et al., 2010).

Traditionally, Biome-BGC uses the empirical, multiplicative Jarvis method for stomatal conductance calculations (Jarvis, 1976). In this method, stomatal conductance is calculated as the product of the maximum stomatal conductance (model parameter) and limiting stress functions based on minimum temperature, VPD, and soil water status (Trusilova et al., 2009).

In BBGCMuSo, we kept this logic as its applicability was demonstrated in many studies (see Introduction). In contrast to the original model, the stress function of soil water status is currently based on relative soil water content and the introduced SMSI (instead of soil water potential) (Hidy et al., 2012). Beyond this, we modified the original method of calculation to take into account the changes in ambient CO_2 concentration. It was demonstrated that the stomatal response of Biome-BGC to increasing atmospheric CO_2 concentration is not consistent with observations (Sándor et al., 2015; note that the latter study used BBGCMuSo 2.2 for which the modification was not yet implemented). Therefore, we implemented an additional multiplicative factor in the calculations in BBGCMuSo 4.0.

In Biome-BGC, stomatal conductance is the function of maximum stomatal conductance (that is an input ecophysiological parameter) and a set of limitation factors. These multiplicative limitation factors summarize the effects of SWC, minimum soil temperature, VPD, and photosynthetic photon flux density. As we mentioned above (Sect. 3.2.1), we modified the limitation function of SWC on stomatal conductance. Besides this modification, a new CO_2 concentration-dependent adjustment factor was implemented in order to improve stomatal calculation based on Franks et al. (2013). They demonstrated a significantly similar dependence of stomatal conductance on ambient CO_2 concentration from hourly to geological timescales. Though the Franks et al. (2013) paper presents results for stomatal conductance in general (as opposed to maximum stomatal conductance), we use the assumption that the same function describes changes in maximum stomatal conductance as well. This assumption is acceptable since stomatal conductance has an upper limit which is present in conditions without environmental stress and with maximum illumination.

In our approach, data from Franks et al. (2013; Table S1 in their Supplement) were used to fit a power function to describe the quantitative relationship between relative change of stomatal conductance ($g_{\mathrm{w(rel)}}$; in fact, this is stomatal conductance to water vapor but this is proportional to stomatal

conductance to CO_2) to changes of ambient CO_2 mixing ratio (Fig. 7b in Franks et al., 2013). The changes are expressed relative to standard conditions:

$$g_{w(rel)} = 39.43 \cdot [CO_2]^{-0.64}, \quad (16)$$

where $[CO_2]$ is atmospheric CO_2 mixing ratio in ppm. In BBGCMuSo v4.0, maximum stomatal conductance is first recalculated according to the actual CO_2 concentration (the latter is supplied by the user for each simulation year). As maximum stomatal conductance is no longer constant (which was the case in the original Biome-BGC and also in BBGCMuSo up to version 3.0), it is assumed that the maximum stomatal conductance defined by the user represents end of the 20th century conditions (at $\sim$ 360 ppm mixing ratio representing $\sim$ year 1995 conditions; g_{smax_EPC}).

To calculate actual maximum stomatal conductance, first $g_{w(rel)}$ is calculated at 360 ppm according to Eq. (13) ($g_{w(rel)[360\,ppm]} = 39.43 \times 360^{-0.64} = 0.9116$; note that this value is not exactly 1 because of the scatter of data used to fit the power function). Next, $g_{w(rel)}$ is calculated for the given $[CO_2]$ value according to Eq. (16). The final maximum stomatal conductance (g_{smax}) is calculated as

$$g_{smax} = g_{w(rel)} \,/\, 0.9116 \cdot g_{smax_EPC}. \quad (17)$$

The final maximum stomatal conductance is used for subsequent calculations for evapotranspiration and photosynthesis. This modification is essential for climate-change-related simulations.

4.4 Modification in the model run

4.4.1 Dynamic mortality

Annual whole-plant mortality fraction (WPM) is part of the ecophysiological parameterization of Biome-BGC (user-supplied value) which is assumed to be constant throughout the simulation. From the point of view of forest growth, constant mortality can be considered a rough assumption. Ecological knowledge suggests that WPM varies dynamically within the life cycle of forest stands due to competition for resources or due to competition within tree species (plus many other causes; Hlásny et al., 2014).

In order to enable more realistic forest stand development simulation, we implemented an option for supplying annually varying WPM to BBGCMuSo (this option can also be used with other biome types with known, annually varying disturbance levels). During the normal phase of the simulation, the model can either use constant mortality or it can use annually varying WPM defined by the user. Technical details about the application of this option can be found in Sect. 3.6 of the BBGCMuSo v4.0 user guide (Hidy et al., 2015).

4.4.2 Optional transient run

Model spinup in Biome-BGC typically represents steady-state conditions before the industrial revolution (without changing atmospheric CO_2 concentration and N deposition). Therefore, the usual strategy for spinup is to use constant (preindustrial) CO_2 and N_{dep} values during the spinup followed by annually varying values for the entire normal simulation (representative of present-day conditions or 20th century conditions). This strategy might be used due to unknown site history or a lack of driving data. However, this logic can lead to undesired transient behavior of the model results as the user may introduce a sharp change by the inconsistent CO_2 and/or N_{dep} data between the spinup and normal phase (note that both CO_2 and N_{dep} are important drivers of plant growth).

In order to avoid this phenomena (and more importantly, to take into account site history), some model users performed one or more transient simulations to enable smooth transition from one simulation phase to the other (mainly, from the spinup phase to the normal phase; Thornton et al., 2002; Vetter et al., 2005; Hlásny et al., 2014). However, this procedure means that the users have to perform a third model run (and sometimes even more) using the output of the spinup phase, and create the input that the normal phase can use.

In BBGCMuSo, we implemented a novel approach to eliminate the effect of sharp changes in the environmental conditions between the spinup and normal phase. According to the modifications, now it is possible to make an automatic transient simulation after the spinup phase.

To initiate the transient run, the user can adjust the settings of the spinup run. If needed, a regular spinup will first be performed with constant CO_2 and N deposition values followed by a second run to be performed using the same meteorological time series defined for the spinup. In this way, the length of the transient run is always equal to the length of the meteorology data used for the spinup phase. During the transient run, annually varying CO_2 concentration data can be used (but they should be constructed to provide a transition from preindustrial to industrial CO_2 concentrations). Utilization of annually varying N-deposition data is optional but it is preferred. The input data of transient run are the output of the spinup phase, and the output data of the transition run are the input of the normal phase. Technical details about the transient run can be found in Sect. 2.2 of the user guide (Hidy et al., 2015).

As management might play an important role in site history (and consequently in biogeochemical cycles), the new transient simulation in BBGCMuSo can include management in an annually varying fashion (management is described below).

4.4.3 Land-use-change simulations

Another new feature was added to BBGCMuSo that is also related with the proper simulation of site history. As the spinup phase is usually associated with preindustrial conditions, the normal phase might represent a plant functional type that is different from the one present in the spinup phase.

For example, present-day croplands can occupy land that was originally forest or grassland, so in this case spinup will simulate forest in equilibrium, and then the normal phase will simulate croplands. Another example is the simulation of afforestation that might require spinup for grasslands, and normal phase for woody vegetation. We may refer to these scenarios as land use change (LUC) related simulations.

One problem that was associated with LUC in earlier model versions was the frequent crash of the model with the error "negative nitrogen pool" during the beginning of the normal phase. This error was typical if the spinup and normal ecophysiological parameterization differed in terms of plant C : N ratios and could occur for some of the plant actual, transfer, and storage pools (e.g., leaf, fine root, soft stem, fruit, live root, dead root, live stem, or dead stem). Equilibrium pools of soil C and N, which are the most important elements for the initial conditions of the normal run, did not suffer from this error.

In order to avoid the negative nitrogen pool error, we have implemented the following automatic procedure in BBGCMuSo. According to the changes, after the spinup phase has ended, only the equilibrium plant C pools are passed to the normal phase. The plant nitrogen pools are calculated by the model code, so that the resulting C : N ratios are harmonized with the C : N ratio of the different plant compartments presented in the ecophysiological parameterization of the normal phase. This modification means that spinup plant nitrogen pools are not passed to the normal phase, but in fact this is not needed because LUC means change in the existing plant functional type, so new plant C : N ratios will inevitably be realized. Implementation of this routine has enabled that LUC and site history can be simulated properly.

4.5 Empirical estimation of other greenhouse gases

Quantification of the full greenhouse gas (GHG) balance of ecosystems was not possible with the original Biome-BGC. Non-CO_2 greenhouse gases (GHGs) are important elements of the biogeochemistry of the soil–plant system. Nitrous oxide (N_2O) and methane (CH_4) are strong GHGs that can eventually compensate the CO_2 sink capacity of ecosystems resulting in GHG-neutral or GHG-source activity (Schulze et al., 2009). We established the first steps towards improved modeling possibilities with Biome-BGC that includes soil efflux estimation of non-CO_2 GHGs.

4.5.1 Estimation of nitrous oxide and methane flux of unmanaged soil

Due to their importance, an empirical estimation of N_2O and CH_4 emission from soils was implemented in BBGCMuSo based on the method of Hashimoto el al. (2011). Gas fluxes are described in terms of three functions: soil physiochemical properties (C : N ratio for N_2O; bulk density of top soil layer for CH_4), water-filled pore space (WFPS) of top soil layer, and soil temperature of top soil layer.

The Hashimoto et al. (2011) method was developed for unmanaged ecosystems. We adapted it to managed ecosystems by including emission estimates from livestock and manure management using Tier 1 methods of IPCC (2006).

4.5.2 Estimation of nitrous oxide and methane flux from grazing and fertilizing

The IPCC (2006) Tier 1 method was implemented in BBGCMuSo to give a first estimation to CH_4 and N_2O emissions due to grazing and fertilizing.

Due to their large population and high CH_4 emission rate, cattle are an important source of CH_4. Methane emissions of cattle originate from manure management (including both dung and urine) and enteric emissions. Methane emission from enteric fermentation is estimated using the number of the animals and the region-specific methane emission factor from enteric fermentation (IPCC, 2006; Ch. 10, Table 10.11). Another mode of methane production is the emission during the storage of manure. Methane emission from manure management is estimated using the number of animals and the region-specific methane emission factor from manure management (IPCC, 2006; Ch. 10, Table 10.14).

In summary, the flux of the methane (F_{CH_4}; $\mathrm{mg\,CH_4\,m^{-2}\,day^{-1}}$) is the sum of soil flux, flux from fermentation, and from manure management:

$$\left(F_{CH_4}\right)_{\mathrm{total}} = \left(F_{CH_4}\right)_{\mathrm{soil}} + \left(F_{CH_4}\right)_{\mathrm{fermentation}} + \left(F_{CH_4}\right)_{\mathrm{manure}}. \quad (18)$$

The emissions of N_2O that result from anthropogenic N inputs or N mineralization occur through both direct pathways (directly from the soils to/from which the N is added/released – grazing and fertilization), and through indirect pathways (volatilization, biomass burning, and leaching). Volatilization fluxes were already implemented into BBGCMuSo. Direct emissions of N_2O from managed soils consist of the emission from animal excretion and from fertilization. The former is estimated by multiplying the total amount of N excretion by an emission factor for that type of manure management system (IPCC, 2006; Ch. 10, Table 10.21). The latter is estimated using emission factors developed for N_2O emissions from synthetic fertilizer and organic N application (IPCC, 2006; Ch. 11, Table 10.21).

In summary, the flux of the nitrous oxide (F_{N_2O}; $\mathrm{mg\,N_2O\,m^{-2}\,day^{-1}}$) is the sum of soil flux, flux from fermentation, and from manure management:

$$\left(F_{N_2O}\right)_{\mathrm{total}} = \left(F_{N_2O}\right)_{\mathrm{soil}} + \left(F_{N_2O}\right)_{\mathrm{grazing}} + \left(F_{N_2O}\right)_{\mathrm{fertilizing}} \quad (19)$$

5 Simulation results: model evaluations

In order to examine and evaluate the functioning of BBGC-MuSo, case studies are presented in this section regarding different vegetation types: C_3 grassland (Bugac, Hungary), C_4 maize (Mead, Nebraska, USA), and C_3 oak forest (Jastrebarsko, Croatia).

The model behavior is evaluated by visual comparison of measured and simulated data and by quantitative measures such as root mean squared error (RMSE), normalized root mean squared error (NRMSE; weighted by the difference of maximum and minimum of the measured data), bias (average difference between simulated and measured variables, where positive bias means systematic overestimation and negative bias means overall underestimation), coefficient of determination (R^2) of the regression between measured and modeled data, and the Nash–Sutcliffe modeling efficiency (NSE). The range of NSE is between 1.0 (perfect fit) and $-\infty$. An efficiency of lower than 0 means that the mean of the observed time series would have been a better predictor than the model. NSE and R^2 are dimensionless. The dimension of RMSE and bias is the dimension of the variable to which it refers. The dimension of NRMSE is %.

In this study, model parameters were taken from the literature, and also from previous parameterization of Biome-BGC. For the newly introduced parameters, we use values that provided reasonable results during model development. The number of parameters in the original model (Biome-BGC v4.1.1 MPI) and BBGCMuSo (Biome-BGCMuSo v4.0) is not the same (MuSo has more ecophysiological parameters than the original model, while a few parameters of the original model are no longer used in BBGCMuSo) but the same values were set in the case of common parameters.

The simulation results of the original Biome-BGC and BBGCMuSo are compared to the measurements. Different model features such as the senescence mechanism, management, and groundwater effects are illustrated in the Supplement (Sects. S2–S9).

BBGCMuSo has more than 600 different output variables. In this study, we focus on the variables relevant for the evaluation of model performance: GPP, TER, net ecosystem exchange (NEE), LHF, LAI, C content of aboveground biomass (abgC), and SWC in the 10–30 cm soil layer.

5.1 C3 grassland/pasture

Measured data at Bugac are available from 2003 to 2015. In order to present model behavior, only three consecutive years were selected (2009–2011) that represented different meteorological conditions. In 2009, the annual sum of precipitations was 14 % lower, and mean annual temperature was 10 % higher than the long-term mean. In 2010, precipitation was 65 % higher and temperature was near average (2 % lower). In 2011, precipitation was 22 % lower than average and temperature was close to the long-term mean.

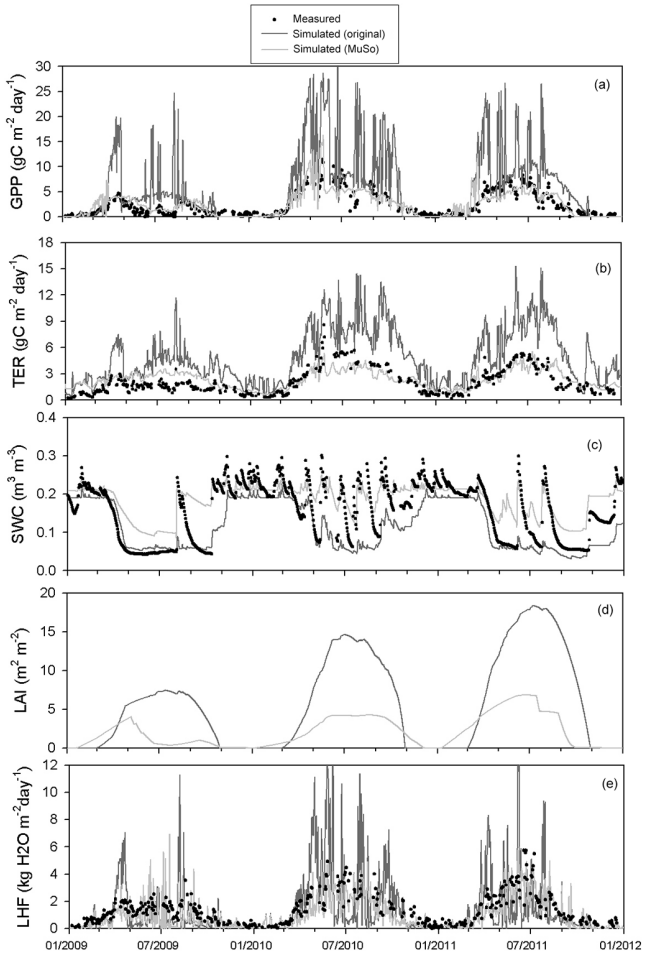

Figure 6. Measured (black dots) and simulated variables **(a)** GPP, **(b)** TER, **(c)** SWC, **(d)** LAI, **(e)** LHF using the original Biome-BGC (dark grey lines) and BBGCMuSo (light grey lines) models for grassland at the Bugac site between 2009 and 2011. Measured LAI was not available at Bugac.

For the Bugac simulation, several novel features were used from BBGCMuSo v4.0. The HSGSI-based phenology, transient simulation, drought-related plant senescence, standing dead biomass pool, grazing settings (see Hidy et al., 2015 for grazing-related input data), non-zero soft stem allocation, management-related decrease of storage and the actual pool, and acclimation were all used in the simulation.

Both during spinup and normal phase of the simulation, we assumed that the vegetation type is grassland; therefore, the C_3 grass parameterization was used (see the Supplement Table S1 for parameterization).

Figure 6 shows that the original Biome-BGC overestimates GPP, TER, LAI, and LHF. Due to the implementation of grazing and plant senescence processes, the overestimation of GPP, TER, and LHF were decreased at the Bugac site where drought is a common phenomenon. The average observed maximum LAI is about 4–5 $m^2\ m^{-2}$ at Bugac. There-

fore, due to model improvements, simulated LAI is more realistic using BBGCMuSo. This was possible due to the implementation of the new soft stem pool that now can contain part of the aboveground C (in the original model, all aboveground C formed leaf biomass for grasses).

It is notable that BBGCMuSo estimates an onset of vegetation growth that is too early, though measured LAI is not available for the studied years. Given the climate of the Bugac site, intensive spring growth is expected to start around the beginning of March (Nagy et al., 2007, 2011) which is not reproduced by the BBGCMuSo simulations presented in Fig. 6d (for the original Biome-BGC prescribed, fixed start dates are used due to well-recognized problems with the original grass phenology routine; see Hidy et al., 2012). BBGCMuSo uses the HSGSI method (see Sect. 4.3.1) to estimate onset and offset of the growing season. In the presented simulation, HSGSI parameter settings (most importantly the heat sum limit) were not adjusted, which resulted in an onset that was too early due to warmer periods in the beginning of 2009 and 2010. Optimization of the HSGSI driving parameters might resolve this issue.

Model evaluation results of the Bugac site using the original Biome-BGC and the BBGCMuSo. The statistical indicators show that with the exception of SWC, the simulation quality typically improved with BBGCMuSo. BBGCMuSo-simulated LHF has higher bias (in absolute sense) than the original model, but the other error metrics perform better. It is notable that NSE became positive for GPP, TER, and LHF while it was negative for all three variables with the original Biome-BGC.

The SWC estimation by the original model was closer to the observations than the result with BBGCMuSo. However, as the original Biome-BGC has a simple, one-layer bucket module for soil hydrology, SWC estimation by the original model and topsoil SWC simulation by Biome-BGCMuSo are not comparable. SWC provided by the original model has no vertical profile, which means that it is not expected that the simulation will match observation. Nevertheless, although the errors are higher in the case of BBGCMuSo (RMSE, NRMSE, NSE, BIAS), the correlation is higher. This is relevant because in the BBGCMuSo simulation, the relative change of soil water content significantly impacts the senescence and decomposition fluxes (see Sect. 3.2). Therefore, if the relative change of the soil water content is realistic, the soil moisture limited processes can still be realistic in spite of the obvious bias in the measurements.

The Supplement Sect. S2 contains additional simulation results for Bugac demonstrating the effect of the long-lasting drought on plant state, the senescence effect on plant processes and carbon balance, and the effect of grazing.

5.2 C4 cropland

Measured data and simulated results are presented for the 2003–2006 period for the Mead1 site (Fig. 7).

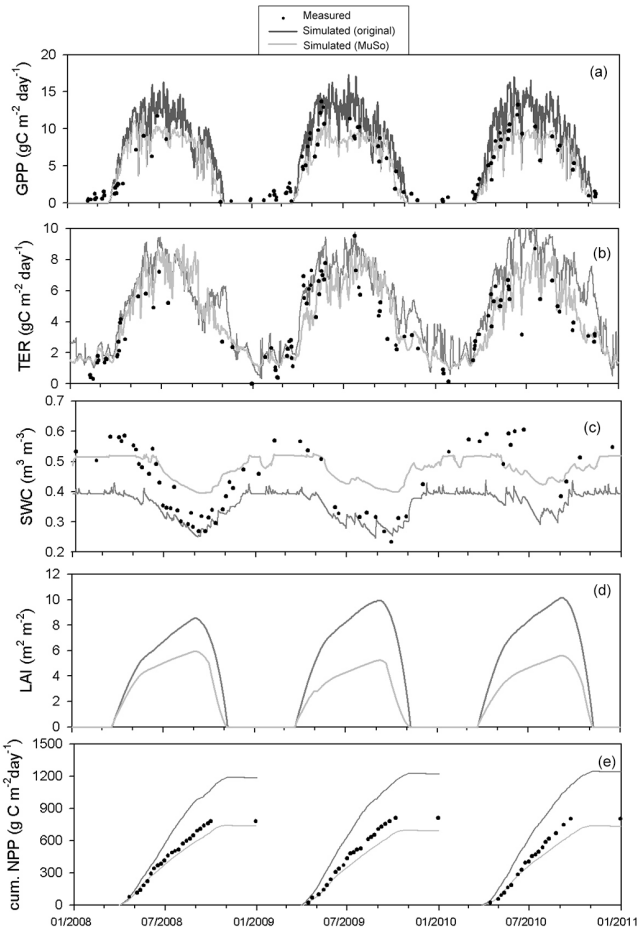

Figure 7. Measured (black dots) and simulated variables **(a)** GPP, **(b)** TER, **(c)** SWC, **(d)** LAI, **(e)** abgC using original Biome-BGC (dark grey lines) and BBGCMuSo (light grey lines) models for maize simulation at the Mead1 site between 2003 and 2006.

For Mead, the applied novel features with BBGCMuSo included C_4 enzyme-driven photosynthesis, transient simulation, planting, harvest, irrigation, drought-related plant senescence, genetically programmed leaf senescence, standing dead biomass pool, fruit pool (in this case, maize yield), non-zero soft stem allocation, and acclimation. Note that the allocation-related "current growth proportion" parameter that controls the content of the storage pool (non-structured carbohydrate reserve for next year's new growth) was zeroed here in order to avoid natural plant growth in the spring. In other words, in the case of planting, the storage pool has to be turned off as maize growth is only possible after sowing.

During the spinup phase, we assumed that the vegetation type was grassland before cropland establishment. Therefore, C_3 grass parameterization was used. In the normal phase, maize parameterization was used. Note that change in ecophysiological parameterization was possible due to the developments (see Sect. 2). The Supplement Table S1 contains the complete parameterization for the maize simulation.

As noted (Sect. 3.5.2), there is a high chance for model error if the spinup and normal ecophysiological parameterization differ in terms of plant C : N ratios (due to the internal model logic). To avoid this error, in the case of original Biome-BGC, the C : N ratios of maize were used in the spinup phase. Mead1 is under management including irrigation, fertilization, harvest, and ploughing. The original model assumes that the vegetation is undisturbed, so no management practices could be set. For BBGCMuSo, management was set according to information taken from the site PI.

Figure 7 shows that the original model underestimated GPP in the vegetation period (in contrast to BBGCMuSo) because it cannot take into account the effect of irrigation and fertilization, which support the growth of agricultural crops. The original model overestimated GPP following harvest because plant material was not removed from the site. Using BBGCMuSo, the overestimation of TER and LAI decreased compared to the original model due to the simulated harvest. For BBGCMuSo, this overestimation decreased also due to the novel fruit and soft stem simulations (in the original model, aboveground plant material apportions biomass to leaves only).

The measurement results from the Mead1 site show that abgC and LAI are decoupled after the initial growth, as LAI decreases, but abgC still increases after the beginning of July. This means that LAI saturates earlier than biomass growth, but this pattern is not reflected by the models' results, because abgC and LAI follow similar trends. This unrealistic behavior is likely the consequence of the static allocation parameterization.

The results of the quantitative model evaluation are presented in Table 4 for Mead using the original Biome-BGC and the BBGCMuSo. According to the error metrics, the simulation quality improved due to the model developments for GPP, TER, LAI and abgC, and also for SWC. For BBGCMuSo, the squares of correlation are higher and the errors (both RMSE and bias) are smaller than in the case of the original model using the original parameters. Values of NSE are close to 1.0 using BBGCMuSo, indicating a good match of the modeled values and the observed data. For the original model, NSE values are much smaller or negative. NSE is negative for SWC both for the original and the BBGCMuSo version in spite of the lower bias of the latter. Again, due to the very simplistic SWC module of the original model, its SWC results are not directly comparable with observations.

The Supplement Sect. S3 presents additional simulation results for the Mead1 site, demonstrating the effect of new model developments like irrigation fertilization, and the genetically programmed leaf senescence.

5.3 Deciduous broad-leaved forest

For the Jastrebarsko forest site, measurement data were available for the period from 2008 to 2014. But, as the measurement height was changed in spring 2011 (flux tower was upgraded due to tree growth), to assure the homogeneity of the measurement data we used data from 2008–2010 only.

For simulation at Jastrebarsko, several novel features were used from BBGCMuSo v4.0. For example, transient simulation, alternative tipping bucket soil water balance calculation, groundwater effect on stomatal conductance and decomposition, drought-related plant senescence, thinning, fruit allocation, bulk denitrification, soil moisture limitation calculation, soil stress index, soil texture change through the soil profile, and respiration acclimation were all used in the simulation. We also used the possibility to adjust the parameter for maintenance respiration, which is fixed within the source code in the original Biome-BGC model. We used the value of $0.4\,\mathrm{kg\,C\,kg\,N^{-1}\,day^{-1}}$ based on newly available data (Cannell and Thornley, 2000).

During both the spinup and normal phases, we assume that the vegetation type was pedunculate oak forest; therefore, oak parameterization was used (see the Supplement Table S1 for parameterization).

Figure 8 shows that the original Biome-BGC overestimates GPP, TER, NPP, and LAI. The probable reason for this is high N-fixation parameter value, estimated to $0.0036\,\mathrm{g\,N\,m^{-2}\,yr^{-1}}$, resulting from the presence of N-fixer species *Alnus glutinosa* (see the Supplement for details) and, at the same time, the lack of denitrification process in the original Biome-BGC version. Due to the implementation of dry and wet bulk denitrification processes, effects of groundwater, and soil moisture stress in the BBGCMuSo version, the overestimation of GPP, TER, and NPP was no longer present and simulation results significantly improved. The Jastrebarsko forest site is a lowland oak forest with complex soil hydrology which cannot easily be simulated using a simple soil bucket approach, as it is a case in original Biome-BGC model. Soil at the Jastrebarsko site is Stagnic Luvisol, with an impermeable clay horizon at 2–3 m depth and poor vertical water conductivity, resulting with parts of the forest being partly waterlogged or even flooded with stagnating water during winter and early spring. Flooding leads to increased denitrification (Groffman and Tiedje, 1989; Kulkarni et al., 2014) and, in combination with hypoxic conditions in the root zone, reflects negatively on GPP and TER (Fig. 8a,b).

Soil water content simulation in BBGCMuSo version shows improvement for the leaf-off season (November–April) when, unlike the original version, soil water saturation in BBGCMuSo simulation becomes evident (Fig. 8c). BBGCMuSo still overestimates soil moisture status in the summer. According to the original Biome-BGC, the forest never experiences soil saturation, which is contrary to the actual situation in winter and early spring. The original Biome-BGC provides only SWC data for one layer of the entire rooting zone (0–100 cm in this case), and therefore it cannot be directly compared with the actual measurements or output from BBGCMuSo which correspond to the 0–30 cm soil layer. Also, it should be emphasized that the parameters

Table 3. Quantitative evaluation of the original and adjusted models at the grassland site in Bugac using different error metrics. ORIG means the original Biome-BGC, while MuSo refers to the BBGCMuSo. See text for the definitions of the error metrics.

	R^2		RMSE		NRMSE		NSE		Bias	
	ORIG	MuSo	ORIG	MuSo	ORIG	MuSo	ORIG	MuSo	ORIG	MuSo
GPP	0.50	0.66	5.82	1.52	51.2	13.4	−4.78	0.61	2.81	0.11
TER	0.65	0.64	3.21	0.98	38.1	11.6	−3.59	0.57	2.47	0.33
LHF	0.24	0.62	1.89	0.83	33.2	14.5	−1.51	0.52	0.01	−0.33
SWC	0.60*	0.64	0.04*	0.09	34.6*	87.7	−0.46*	−8.3	−0.01*	0.09

* SWC simulated by the original Biome-BGC represents constant value within the entire root zone.

Table 4. Quantitative model evaluation regarding maize simulation at the Mead1 site using different error metrics. ORIG means the original Biome-BGC, while MuSo refers to the BBGCMuSo. See text for the definitions of the error metrics.

	R^2		RMSE		NRMSE		NSE		Bias	
	ORIG	MuSo	ORIG	MuSo	ORIG	MuSo	ORIG	MuSo	ORIG	MuSo
GPP	0.61	0.87	5.83	3.44	19.0	11.1	0.58	0.86	−0.41	−0.91
TER	0.59	0.86	4.65	1.75	35.4	13.3	−0.58	0.78	3.8	−0.83
SWC	0.12*	0.01	0.13*	0.09	41.2*	30.1	−4.53*	−1.94	0.12*	0.07
LAI	0.26	0.59	5.81	1.61	97.6	27.1	−7.03	0.91	4.22	−0.01
abgC	0.36	0.82	296.5	159.6	27.4	14.8	0.17	0.76	−129.1	7.9

* SWC simulated by the original Biome-BGC represents constant value within the entire root zone.

of soil bulk density, SWC of saturation, field capacity, and wilting point for soil layers were not available. BBGCMuSo calculated those parameters based only on the provided parameters for soil texture.

Simulated LAI value also decreased to more realistic values in BBGCMuSo due to model improvements (Fig. 8d). Based on litterfall data ($0.408\,kg\,m^{-2}$; Marjanović et al., 2011b) and average specific leaf area of $15\,m^2\,kg^{-1}$ for oak (Morecroft and Roberts, 1999), the average maximum LAI at Jastrebarsko is estimated to be $6.1\,m^2\,m^{-2}$, just slightly above what is estimated by BBGCMuSo. BBGCMuSo NPP estimates are also in good agreement with those from field observation (Marjanović et al., 2011a), unlike those of the original version which overestimate NPP (Fig. 8e).

The results of the quantitative model evaluation are presented in Table 5 for the Jastrebarsko site using the original Biome-BGC and the BBGCMuSo. The quality of simulation usually improved with BBGCMuSo due to the model developments (R^2 for SWC is an exception, but see the notes above about the SWC simulation of the original Biome-BGC). Key variables' errors and biases are smaller in comparison to the original model using the original parameter set.

The Supplement Sect. S4 contains additional simulation results for the Jastrebarsko site demonstrating the effect of new model developments.

6 Discussion and conclusions

Biogeochemical models inevitably need continuous development to improve their ability to simulate ecosystem C balance. In spite of the considerable development in our understanding of the C balance of terrestrial ecosystems (Baldocchi et al., 2001; Friend et al., 2006; Williams et al., 2009), current biogeochemical models still have inherent uncertainties. The major sources of uncertainties are internal variability, initial and boundary conditions (e.g., equilibrium soil organic matter pool estimation), parameterization, and model formulation (process representation) (Schwalm et al., 2015; Sándor et al., 2016).

In this study, our objective was to address model-structure-related uncertainties in the widely used Biome-BGC model.

The interactions between water availability and ecosystem C balance are widely documented in the literature. In a recent study, Ahlström et al. (2015) showed that semi-arid ecosystems have strong contribution to the trend and interannual variability of the terrestrial C sink. This finding emphasizes the need to accurately simulate soil-water-related processes and plant senescence due to prolonged drought. In earlier model versions, drought could not cause plant death (i.e., LAI decrease) which resulted in a quick recovery of the vegetation after a prolonged drought. In our implementation, long-lasting drought can cause irreversible plant senescence which is more realistic than the original implementation.

The role of management as the primary driver of biomass production efficiency in terrestrial ecosystems was shown

Table 5. Quantitative model evaluation of simulation for deciduous broad-leaved forest for the Jastrebarsko forest site using different error metrics. ORIG means the original Biome-BGC, while MuSo refers to the BBGCMuSo. See text for the definitions of the error metrics.

	R^2		RMSE		NRMSE		NSE		Bias	
	ORIG	MuSo	ORIG	MuSo	ORIG	MuSo	ORIG	MuSo	ORIG	MuSo
GPP	0.84	0.84	3.67	1.77	27.3	13.1	−0.13	0.74	2.27	0.33
TER	0.81	0.83	2.5	1.31	27.4	14.4	−0.51	0.59	2.13	0.82
SWC	0.83*	0.67	0.11*	0.08	27.1*	21.2	0.06*	0.42	−0.08*	0.02
NPP	0.99	0.99	240.9	70.3	30.5	8.9	−0.03	0.91	220.3	−52.3

* SWC simulated by the original Biome-BGC represents constant value within the entire root zone.

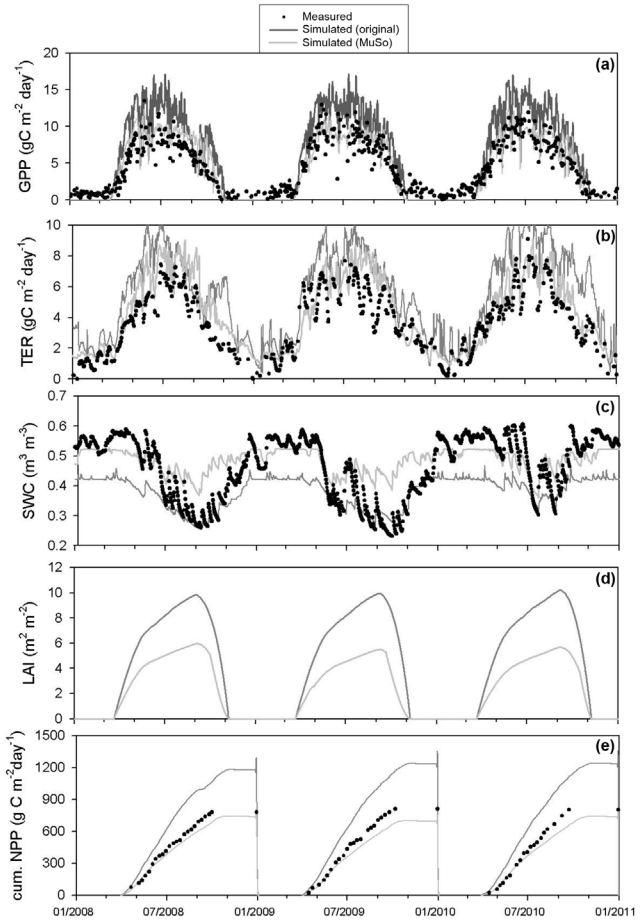

Figure 8. Measured (black dots) and simulated variables using original Biome-BGC (dark grey lines) and BBGCMuSo (light grey lines) regarding deciduous broad-leaved forest at the Jastrebarsko site between 2008 and 2010. **(a)** GPP, **(b)** TER, **(c)** SWC (note: original Biome-BGC provides simulation results only for one layer, namely "the rooting depth", which is 0–100 cm in this case), **(d)** LAI, **(e)** cumulative NPP. Note that measured LAI is not available.

by Campioli et al. (2015). The study clearly demonstrates that management cannot be neglected if proper representation of the ecosystem C balance is needed. The management modules built into BBGCMuSo cover, on a global basis, the majority of human interventions in managed ecosystems. As management practices require prescribed input data for BBGCMuSo, accuracy of the simulations will clearly depend on the quality of management description which calls for proper data to drive the model.

Representation of acclimation of plant respiration and photosynthesis was shown to be one major uncertainty in global biogeochemical models (Lombardozzi et al., 2015). We introduced acclimation of autotrophic respiration in BBGCMuSo, which is a major step towards more realistic climate-change-related simulations. Representation of photosynthesis acclimation (Medlyn et al., 2002) is needed in future modifications as another major development.

Due the implementation of many novel model features, the model logic became more complex. Thus, process interactions became even more complicated, which means that extensive testing is needed to find problems and limitations.

The earlier version of BBGCMuSo (v2.2) was already used in a major model intercomparison project (FACCE MACSUR – Modelling European Agriculture with Climate Change for Food Security, a FACCE JPI knowledge hub; Ma et al., 2014; Sándor et al., 2016). Within MACSUR, nine grassland models were used and their performance was tested against EC and biomass measurements. BBGCMuSo v2.2 results were comparable with other models like LPJmL, CARAIB, STICS, EPIC, PaSim, and others. In spite of the successful application of the predecessor of BBGCMuSo v4.0, SWC simulations were still problematic (Sándor et al., 2016). Developments are clearly needed in terms of soil water balance and ecosystem-scale hydrology in general.

Other developments are still needed to improve simulations with dynamic C and N allocation within the plant compartments (Friedlingstein et al., 1999; Olin et al., 2015). Complete representation of ammonium and nitrate pools with associated nitrification and denitrification is also needed to avoid ill-defined, N balance-related parameters (Thomas et al., 2013). Even further model development will require

the addition of other nutrient limitations (phosphorus, potassium).

Static allocation of C and N into the plant compartments is still present in BBGCMuSo, with a novel modification that uses GDD to initiate fruit allocation. Unrealistic coupling of aboveground biomass and LAI for the Mead simulation demonstrated the need to implement more flexible dynamic allocation. We plan to extend BBGCMuSo using the logic of the traditional crop models like DSSAT (Ritchie, 1998) where GDD-dependent allocation is implemented, and retranslocation of leaf C to fruit C is also realized during grain filling.

The Bugac case study demonstrated that the phenology module needs optimization to capture the observed onset of vegetation growth. This requires deeper evaluation of the HSGSI routine in multiple plant functional types. Extension of the HSGSI module might be also needed in the future.

In the present paper, three case studies were presented to demonstrate the effect of model structural improvements on the simulation quality. Clearly, extensive testing is required at multiple EC sites to evaluate the performance of the model and to make adjustments if needed.

Parameter uncertainty also needs further investigations. Model parameterization based on observed plant traits is possible today thanks to new data sets (e.g., White et al., 2000; Kattge et al., 2011; van Bodegom et al., 2012). However, in some cases, imperfect model structure may cause distortion owing to compensation of errors (Martre et al., 2015). Additionally, plant traits (e.g., specific leaf area, leaf C : N ratio, photosynthesis-related parameters) vary considerably in space, so even though plant trait data sets are available, they might not capture the site-level parameters. These issues raise the need for proper infrastructure for parameter estimation (or, in other words, calibration or model inversion). The need for model calibration is also emphasized as we introduced a couple of empirical parameters in BBGCMuSo (e.g., those related to plant senescence, water stress thresholds, denitrification drivers, disturbance-related mortality parameters) that need optimization using measurement data from multiple sites. In other words, though BBGCMuSo parameterization is mostly based on observable plant traits, model calibration can not be avoided in the majority of the cases (Hidy et al., 2012).

To address this problem we created a computer-based open infrastructure based on the workflow concept that can help a wide array of users in the application of the new model. The infrastructure is similar to PEcAn (Dietze et al., 2014) which is a collection of modules in a workflow that uses the Ecosystem Demography (ED v2.2) model. We followed the concept of model–data fusion (MDF; Williams et al., 2009) when developing the so-called "Biome-BGC Projects Database and Management System" (BBGCDB; http://ecos.okologia.mta.hu/bbgcdb/) and the BioVeL Portal (http://portal.biovel.eu) as a virtual research environment and collaborative tool. BBGCDB and the BioVeL portal help sensitivity analysis and parameter optimization of BBGCMuSo by a computer cluster-based Monte Carlo experiment and GLUE methodology (Beven and Binley, 1992). Further integration is planned using alternative Bayesian calibration algorithms (Hartig et al., 2012) that will provide extended calibration options to the parameters of BBGCMuSo.

We would like to support BBGCMuSo application for the wider scientific community as much as possible. For users of the original Biome-BGC, the question is of course the following: should I move to BBGCMuSo? Does it need a long learning process to move to the improved model? We would like to stress that users of the original Biome-BGC will have a smooth transition to BBGCMuSo, as we mainly preserved the structure of the input files. The majority of changes are related to the seven-layer soil module and to the implementation of management modules. The ecophysiological parameter file is similar to the original but it was extended considerably. This may raise issues but as it is emphasized in our user guide (Hidy et al., 2015), we extended the ecophysiological parameter file with many parameters that will not need adjustment in the majority of the cases. We simply moved some "burned-in" parameters into the ecophysiological parameter in order to allow easy adjustment if needed in the future.

7 Code availability

The source code, the Windows model executable, sample simulation input files, and documentation are available at the BBGCMuSo website (http://nimbus.elte.hu/bbgc). The source code is also available at GitHub (https://github.com/bpbond/Biome-BGC/tree/Biome-BGCMuSo_v4.0).

The Supplement related to this article is available online at doi:10.5194/gmd-9-4405-2016-supplement.

Author contributions. D. Hidy developed Biome-BGCMuSo with modifying Biome-BGC 4.1.1 MPI version. The study was conceived and designed by D. Hidy and Z. Barcza, with assistance from H. Marjanović, G. Churkina, N. Fodor, F. Horváth, and S. Running. It was directed by Z. Barcza and D. Hidy. H. Marjanović, M. Z. Ostrogović Sever, K. Pintér, Z. Nagy, G. Gelybó, L. Dobor, and A. Suyker contributed with simulations, measurement data and their post-processing and ideas on interpretation of the model validation. D. Hidy, Z. Barcza, and H. Marjanović prepared the manuscript and the Supplement with contributions from all co-authors. All authors reviewed and approved the present article and the Supplement.

Acknowledgements. The research was funded by the Hungarian Academy of Sciences (MTA PD 450012), the Hungarian Scientific Research Fund (OTKA K104816), the BioVeL project (Biodiversity Virtual e-Laboratory Project, FP7-INFRASTRUCTURES-2011-2,

project number 283359), the EU FP7 WHEALBI Project (Wheat and Barley Legacy for Breeding Improvement; project No. 613556), the Croatian Science Foundation Installation Research Project EFFEctivity (HRZZ-UIP-11-2013-2492), and metaprogramme Adaptation of Agriculture and Forests to Climate Change (AAFCC) of the French National Institute for Agricultural Research (INRA). We acknowledge the international research project titled "FACCE MACSUR – Modelling European Agriculture with Climate Change for Food Security, a FACCE JPI knowledge hub". Biome-BGC version 4.1.1 (the predecessor of BBGCMuSo) was provided by the Numerical Terradynamic Simulation Group (NTSG) at the University of Montana, Missoula, MT (USA), which assumes no responsibility for the proper use by others. We are grateful to the Laboratory of Parallel and Distributed Systems, Institute for Computer Science and Control (MTA SZTAKI), that provided consultation, technical expertise, and access to the EDGeS@home volunteer desk top grid system in computationally demanding analysis. We thank Ben Bond-Lamberty and one anonymous referee for the valuable comments on the manuscript.

Edited by: T. Kato
Reviewed by: B. Bond-Lamberty and one anonymous referee

References

Ahlström, A., Raupach, M. R., Schurgers, G., Smith, B., Arneth, A., Jung, M., Reichstein, M., Canadell, J. G., Friedlingstein, P., Jain, A. K., Kato, E., Poulter, B., Sitch, S., Stocker, B. D., Viovy, N., Wang, Y. P., Wiltshire, A., Zaehle, S., and Zeng, N.: The dominant role of semi-arid ecosystems in the trend and variability of the land CO_2 sink, Science, 348, 895–899, doi:10.1126/science.aaa1668, 2015.

Alberti, G., Vicca, S., Inglima, I., Belelli-Marchesini, L., Genesio, L., Miglietta, F., Marjanovic, H., Martinez, C., Matteucci, G., D'Andrea, E., Peressotti, A., Petrella, F., Rodeghiero, M., and Cotrufo, M. F.: Soil C:N stoichiometry controls carbon sink partitioning between above-ground tree biomass and soil organic matter in high fertility forests, Iforest 8, 195–206, doi:10.3832/ifor1196-008, 2014.

Atkin, O. K., Atkinson, L. J., Fisher, R. A., Campbell, C. D., Zaragoza-Castells, J., Pitchford, J. W., Woodward, F. I., and Hurry, V.: Using temperature-dependent changes in leaf scaling relationships to quantitatively account for thermal acclimation of respiration in a coupled global climate-vegetation model, Glob. Change Biol., 14, 1–18, doi:10.1111/j.1365-2486.2008.01664.x, 2008.

Aubinet, M., Grelle, G., Ibrom, A., Rannik, U., Moncrieff, J., Foken, T., Kowalski, A. S., Martin, P. H., Berbigier, P., Bernhofer, C., Clement, R., Elbers, J., Granier, A., Grunwald, T., Morgenstern, K., Pilegaard, K., Rebmann, C., Snijders, W., Valentini, R., and Vesala, T.: Estimates of the annual net carbon and water exchange of European forests: the EUROFLUX methodology, Adv. Ecol. Res., 30, 113–175, doi:10.1016/S0065-2504(08)60018-5, 2000.

Baldocchi, D., Falge, E., Gu, L., Olson, R., Hollinger, D., Running, S., Anthoni, P., Bernhofer, C., Davis, K., Evans, R., Fuentes, J., Goldstein, A., Katul, G., Law, B., Lee, X., Malhi, Y., Meyers, T., Munger, W., Oechel, W., Paw U, K. T., Pilegaard, K., Schmid, H. P., Valentini, R., Verma, S., Vesala, T., Wilson, K., and Wofsy, S.: FLUXNET: A new tool to study the temporal and spatial variability of ecosystem-scale carbon dioxide, water vapor, and energy flux densities, B. Am. Meteorol. Soc., 82, 2415–2434, doi:10.1175/1520-0477(2001)082<2415:FANTTS>2.3.CO;2, 2001.

Ball, J. T., Woodrow, I. E., and Berry, J. A.: A model predicting stomatal conductance and its contribution to the control of photosynthesis under different environmental conditions, in: Progress in Photosynthesis Research, edited by: Biggins, J., Springer Netherlands, 221–224, 1987.

Balogh, J., Pintér, K., Fóti, S., Cserhalmi, D., Papp, M., and Nagy, Z.: Dependence of soil respiration on soil moisture, clay content, soil organic matter, and CO_2 uptake in dry grasslands, Soil Biol. Biochem., 43, 1006–1013, doi:10.1016/j.soilbio.2011.01.017, 2011.

Balsamo, G., Beljaars, A., Scipal, K., Viterbo, P., van den Hurk, B., Hirschi, M., and Betts, A. K.: A Revised Hydrology for the ECMWF Model: Verification from Field Site to Terrestrial Water Storage and Impact in the Integrated Forecast System, J. Hydrometeorol., 10, 623–643, doi:10.1175/2008JHM1068.1, 2009.

Barcza, Z., Kern, A., Haszpra, L., and Kljun, N.: Spatial representativeness of tall tower eddy covariance measurements using remote sensing and footprint analysis, Agr. Forest Meteorol., 149, 795–807, doi:10.1016/j.agrformet.2008.10.021, 2009.

Barcza, Z., Bondeau, A., Churkina, G., Ciais, P., Czóbel, S., Gelybó, G., Grosz, B., Haszpra, L., Hidy, D., Horváth, L., Machon, A., Pásztor, L., Somogyi, Z., and Van Oost, K.: Model-based biospheric greenhouse gas balance of Hungary, in: Atmospheric Greenhouse Gases: The Hungarian Perspective, edited by: Haszpra, L., Springer, 295–330, 2011.

Beven, K. and Binley, A.: The future of distributed models: Model calibration and uncertainty prediction, Hydrol. Process., 6, 279–298, doi:10.1002/hyp.3360060305, 1992.

Bond-Lamberty, B., Gower, S. T., Ahl, D. E., and Thornton, P. E.: Reimplementation of the Biome-BGC model to simulate successional change, Tree Physiol., 25, 413–424, doi:10.1093/treephys/25.4.413, 2005.

Bond-Lamberty, B., Gower, S. T., and Ahl, D. E.: Improved simulation of poorly drained forests using Biome-BGC, Tree Physiol., 27, 703–715, doi:10.1093/treephys/27.5.703, 2007a.

Bond-Lamberty, B., Peckham, S. D., Ahl, D. E., and Gower, S. T.: Fire as the dominant driver of central Canadian boreal forest carbon balance, Nature, 450, 89–92, doi:10.1038/nature06272, 2007b.

Campbell, G. S. and Diaz, R.: Simplified soil water balance models to predict crop transpiration, in: Drought Research Priorities for the Drylands, 15–26, 1988.

Campioli, M., Vicca, S., Luyssaert, S., Bilcke, J., Ceschia, E., Chapin III, F. S., Ciais, P., Fernández-Martínez, M., Malhi, Y., Obersteiner, M., Olefeldt, D., Papale, D., Piao, S. L., Peñuelas, J., Sullivan, P. F., Wang, X., Zenone, T., and Janssens, I. A.: Biomass production efficiency controlled by management in temperate and boreal ecosystems, Nat. Geosci., 8, 843–846, doi:10.1038/ngeo2553, 2015.

Cannell, M. G. R. and Thornley, J. H. M.: Modelling the components of plant respiration: Some guiding principles, Ann. Bot.-London, 85, 45–54, doi:10.1006/anbo.1999.0996, 2000.

Chapin, F. S., Woodwell, G. M., Randerson, J. T., Rastetter, E. B., Lovett, G. M., Baldocchi, D. D., Clark, D. A., Harmon, M. E., Schimel, D. S., Valentini, R., Wirth, C., Aber, J. D., Cole, J. J., Goulden, M. L., Harden, J. W., Heimann, M. R., Howarth, W., Matson, P. A., McGuire, A. D., Melillo, J. M., Mooney, H. A., Neff, J. C., Houghton, R. A., Pace, M. L., Ryan, M. G., Running, S. W., Sala, O. E., Schlesinger, W. H., and Schulze, E. D.: Reconciling carbon-cycle concepts, terminology, and methods, Ecosystems 9, 1041–1050, doi:10.1007/s10021-005-0105-7, 2006.

Chen, F. and Dudhia, J.: Coupling an Advanced Land Surface–Hydrology Model with the Penn State–NCAR MM5 Modeling System. Part I: Model Implementation and Sensitivity, Mon. Weather Rev., 129, 569–585, doi:10.1175/1520-0493(2001)129<0569:CAALSH>2.0.CO;2, 2001.

Chiesi, M., Maselli, F., Moriondo, M., Fibbi, L., Bindi, M., and Running, S. W.: Application of BIOME-BGC to simulate Mediterranean forest processes, Ecol. Model., 206, 179–190, doi:10.1016/j.ecolmodel.2007.03.032, 2007.

Churkina, G., Running, S. W., Running, S. W., Schloss, A. L., and the participants of the Potsdam NPP Model Intercomparison: Comparing global models of terrestrial net primary productivity (NPP): the importance of water availability, Glob. Change Biol., 5, 46–55, doi:10.1046/j.1365-2486.1999.00006.x, 1999.

Churkina, G., Tenhunen, J., Thornton, P., Falge, E. M., Elbers, J. A., Erhard, M., Grünwald, T., Kowalski, A. S., Rannik, Ü., and Sprinz, D.: Analyzing the ecosystem carbon dynamics of four European coniferous forests using a biogeochemistry model, Ecosystems, 6, 168–184, doi:10.1007/s10021-002-0197-2, 2003.

Churkina, G., Brovkin, V., von Bloh, W., Trusilova, K., Jung, M., and Dentener, F.: Synergy of rising nitrogen depositions and atmospheric CO_2 on land carbon uptake moderately offsets global warming, Global Biogeochem. Cy., 23, GB4027, doi:10.1029/2008GB003291, 2009.

Churkina, G., Zaehle, S., Hughes, J., Viovy, N., Chen, Y., Jung, M., Heumann, B. W., Ramankutty, N., Heimann, M., and Jones, C.: Interactions between nitrogen deposition, land cover conversion, and climate change determine the contemporary carbon balance of Europe, Biogeosciences, 7, 2749–2764, doi:10.5194/bg-7-2749-2010, 2010.

Ciais, P., Sabine, C., Bala, G., Bopp, L., Brovkin, V., Canadell, J.,Chhabra, A., DeFries, R., Galloway, J., Heimann, M., Jones, C., Le Quéré, C., Myneni, R. B., Piao S., and Thornton, P.: Carbon and Other Biogeochemical Cycles, in: Climate Change 2013: The Physical Science Basis. Contribution of Working Group I to the Fifth Assessment Report of the Intergovernmental Panel on Climate Change edited by: Stocker, T. F., Qin, D., Plattner, G. K., Tignor, M., Allen, S. K., Boschung, J., Nauels, A., Xia, Y., Bex, V., and Midgley, P. M., Cambridge University Press, Cambridge, United Kingdom and New York, NY, USA, 2013.

Clapp, R. B. and Hornberger, G. M.: Empirical equations for some soil hydraulic properties, Water Resour. Res., 14, 601–604, doi:10.1029/WR014i004p00601, 1978.

Collatz, G. J., Ball, J. T., Grivet, C., and Berry, J.: Physiological and environmental regulation of stomatal conductance, photosynthesis and transpiration: a model that includes a laminar boundary layer, Agr. Forest Meteorol., 54, 107–136, doi:10.1016/0168-1923(91)90002-8, 1991.

Damour, G., Simonneau, T., Cochard, H., and Urban, L.: An overview of models of stomatal conductance at the leaf level, Plant. Cell Environ., 33, 1419–1438, doi:10.1111/j.1365-3040.2010.02181.x, 2010.

Dietze, M., Serbin, S., Davidson, C., Desai, A., Feng, X., Kelly, R., Kooper, R., Lebauer, D., Mantooth, J., Mchenry, K., and Wang, D.: A quantitative assessment of a terrestrial biosphere model's data needs across North American biomes, J. Geophys. Res.-Biogeo., 119, 286–300, doi:10.1002/2013JG002392, 2014.

Di Vittorio, A. V., Anderson, R. S., White, J. D., Miller, N. L., and Running, S. W.: Development and optimization of an Agro-BGC ecosystem model for C4 perennial grasses, Ecol. Model., 221, 2038–2053, doi:10.1016/j.ecolmodel.2010.05.013, 2010.

Driessen, P., Deckers, J., Spaargaren, O., and Nachtergaele, F.: Lecture notes on the major soils of the world, edited by: Driessen, P., Deckers, J., Spaargaren, O., and Nachtergaele, F., Food and Agriculture Organization (FAO), 2001.

Eastaugh, C. S., Pötzelsberger, E., and Hasenauer, H.: Assessing the impacts of climate change and nitrogen deposition on Norway spruce (Picea abies L. Karst) growth in Austria with BIOME-BGC, Tree Physiol., 31, 262–274, doi:10.1093/treephys/tpr033, 2011.

Farquhar, G. D., von Caemmerer, S., and Berry, J. A.: A biochemical model of photosynthetic CO_2 assimilation in leaves of C3 species, Planta, 149, 78–90, doi:10.1007/BF00386231, 1980.

Florides, G. and Kalogirou, S.: Annual ground temperature measurements at various depth, available at: https://www.researchgate.net/publication/30500353 (last access: 10 April 2016), 2016.

Fodor, N. and Rajkai, K.: Computer program (SOILarium 1.0) for estimating the physical and hydrophysical properties of soils from other soil characteristics, Agrokémia és Talajt., 60, 27–40, 2011.

Foken, T. and Vichura, B.: Tools for quality assessment of surface-based flux measurements, Agr. Forest Meteorol., 78, 83–105, doi:10.1016/0168-1923(95)02248-1, 1996.

Franks, P. J., Adams, M. A., Amthor, J. S., Barbour, M. M., Berry, J. A., Ellsworth, D. S., Farquhar, G. D., Ghannoum, O., Lloyd, J., McDowel, L., Norby, R. J., Tissue, D. T., and von Caemmerer, S.: Sensitivity of plants to changing atmospheric CO_2 concentration: from the geological past to the next century, New Phytol., 197, 1077–1094, doi:10.1111/nph.12104, 2013.

Friedlingstein, P. and Prentice, I. C.: Carbon-climate feedbacks: a review of model and observation based estimates, Curr. Opin. Environ. Sust., 2, 251–257, doi:10.1016/j.cosust.2010.06.002, 2010.

Friedlingstein, P., Joel, G., Field, C. B., and Fung, I. Y.: Toward an allocation scheme for global terrestrial carbon models, Glob. Change Biol., 5, 755–770, doi:10.1046/j.1365-2486.1999.00269.x, 1999.

Friedlingstein, P., Cox, P., Betts, R., Bopp, L., Von Bloh, W., Brovkin, V., Cadule, P., Doney, S., Eby, M., Fung, I., Bala, G., John, J. J., Jones, C. J., Joos, F., Kato, T. K., Kawamiya, M., Knorr, W., Lindsay, K., Matthews, H. D., Raddatz, T., Rayner, P., Reick, C., Roeckner, E., Schnitzler, K. G., Schnur, R., Strassmann, K., Weaver, A. J., Yoshikawa, C., and Zeng, N.: Climate-carbon cycle feedback analysis: results from the C4MIP model intercomparison, J. Climate, 19, 3338–3353, doi:10.1175/JCLI3800.1, 2006.

Friedlingstein, P., Meinshausen, M., Arora, V. K., Jones, C. D., Anav, A., Liddicoat, S. K., and Knutti, R.: Uncertainties in CMIP5 climate projections due to carbon cycle feedbacks, J. Climate, 27, 511–526, doi:10.1175/JCLI-D-12-00579.1, 2014.

Friend, A. D., Arneth, A., Kiang, N. Y., Lomas, M., Ogée, J., Rödenbeck, C., Running, S. W., Santaren, J. D., Sitch, S., Viovy, N., Woodward, F. I., and Zaehle, S.: FLUXNET and modelling the global carbon cycle, Glob. Change Biol., 1, 1–24, doi:10.1111/j.1365-2486.2006.01223.x, 2006.

Groffman, P. M. and Tiedje, J. M.: Denitrification in north temperate forest soils: Relationships between denitrification and environmental factors at the landscape scale, Soil Biol. Biochem., 21, 621–626, doi:10.1016/0038-0717(89)90054-0, 1989

Hartig, F., Dyke, J., Hickler, T., Higgins, S. I., O'Hara, R. B., Scheiter, S., and Huth, A.: Connecting dynamic vegetation models to data - an inverse perspective, J. Biogeogr., 39, 2240–2252, doi:10.1111/j.1365-2699.2012.02745.x, 2012.

Hashimoto, S., Morishita, T., Sakata, T., Ishizuka, S., Kaneko, S., and Takahashi, M.: Simple models for soil CO_2, CH_4, and N_2O fluxes calibrated using a Bayesian approach and multi-site data, Ecol. Model., 222, 1283–1292, doi:10.1016/j.ecolmodel.2011.01.013, 2011.

Hidy, D., Barcza, Z., Haszpra, L., Churkina, G., Pintér, K., and Nagy, Z.: Development of the Biome-BGC model for simulation of managed herbaceous ecosystems, Ecol. Model., 226, 99–119, doi:10.1016/j.ecolmodel.2011.11.008, 2012.

Hidy, D., Barcza, Z., Thornton, P., and Running, S. W.: User's Guide for Biome-BGC MuSo 4.0, available at: http://nimbus.elte.hu/bbgc/files/Manual_BBGC_MuSo_v4.0.pdf (last access: 15 October 2016), 2015.

Hlásny, T., Barcza, Z., Barka, I., Merganicova, K., Sedmak, R., Kern, A, Pajtik, J., Balazs, B., Fabrika, M., and Churkina, G.: Future carbon cycle in mountain spruce forests of Central Europe: Modelling framework and ecological inferences, Forest Ecol. Manage., 328, 55–68, doi:10.1016/j.foreco.2014.04.038, 2014.

Hunt, E. R., Piper, S. C., Nemani, R., Keeling, C. D., Otto, R. D., and Running, S. W.: Global net carbon exchange and intra-annual atmospheric CO_2 concentrations predicted by an ecosystem process model and three-dimensional atmospheric transport model, Global Biogeochem. Cy., 10, 431–456, doi:10.1029/96GB01691, 1996.

Huntzinger, D. N., Schwalm, C., Michalak, A. M., Schaefer, K., King, A. W., Wei, Y., Jacobson, A., Liu, S., Cook, R. B., Post, W. M., Berthier, G., Hayes, D., Huang, M., Ito, A., Lei, H., Lu, C., Mao, J., Peng, C. H., Peng, S., Poulter, B., Riccuito, D., Shi, X., Tian, H., Wang, W., Zeng, N., Zhao, F., and Zhu, Q.: The North American Carbon Program Multi-Scale Synthesis and Terrestrial Model Intercomparison Project – Part 1: Overview and experimental design, Geosci. Model Dev., 6, 2121–2133, doi:10.5194/gmd-6-2121-2013, 2013.

IPCC: Guidelines for National Greenhouse Gas Inventories, edited by: Eggleston, H. S., Buendia, L., Miwa, K., Ngara, T., and Tanabe, K., National Greenhouse Gas Inventories Programme, IGES, Japan, 2006.

Jarvis, N. J.: A simple empirical model of root water uptake, J. Hydrol., 107, 57–72, doi:10.1016/0022-1694(89)90050-4, 1989.

Jarvis, P. G.: The interpretation of the variations in leaf water potential and stomatal conductance found in canopies in the field, Philos. Trans. R. Soc. B, 273, 593–610, doi:10.1098/rstb.1976.0035, 1976.

Jochheim, H., Puhlmann, M., Beese, F., Berthold, D., Einert, P., Kallweit, R., Konopatzky, A., Meesenburg, H., Meiwes, K. J., Raspe, S., Schulte-Bisping, H., and Schulz, C.: Modelling the carbon budget of intensive forest monitoring sites in Germany using the simulation model BIOME-BGC, iForest – Biogeosciences For., 2, 7–10, doi:10.3832/ifor0475-002, 2009.

Jolly, W., Nemani, R. R., and Running, S. W.: A generalized, bioclimatic index to predict foliar phenology in response to climate, Glob. Change Biol., 11, 619–632, doi:10.1111/j.1365-2486.2005.00930.x, 2005.

Jung, M., Le Maire, G., Zaehle, S., Luyssaert, S., Vetter, M., Churkina, G., Ciais, P., Viovy, N., and Reichstein, M.: Assessing the ability of three land ecosystem models to simulate gross carbon uptake of forests from boreal to Mediterranean climate in Europe, Biogeosciences, 4, 647–656, doi:10.5194/bg-4-647-2007, 2007a.

Jung, M., Vetter, M., Herold, M., Churkina, G., Reichstein, M., Zaehle, S., Ciais, P., Viovy, N., Bondeau, A., Chen, Y., Trusilova, K., Feser, F., and Heimann, M.: Uncertainties of modeling gross primary productivity over Europe: A systematic study on the effects of using different drivers and terrestrial biosphere models, Global Biogochem. Cy., 21, GB4021, doi:10.1029/2006GB002915, 2007b.

Kattge, J., Díaz, S., Lavorel, S., Prentice, I. C., Leadley, P., Bönisch, G., Garnier, E., Westoby, M., Reich, P. B., Wright, I.J., Cornelissen, J. H. C., Violle, C., Harrison, S. P., Van Bodegom, P. M., Reichstein, M., Enquist, B. J., Soudzilovskaia, N. A., Ackerly, D. D., Anand, M., Atkin, O., Bahn, M., Baker, T. R., Baldocchi, D., Bekker, R., Blanco, C. C., Blonder, B., Bond, W. J., Bradstock, R., Bunker, D. E., Casanoves, F., Cavender-Bares, J., Chambers, J. Q., Chapin, F. S., Chave, J., Coomes, D., Cornwell, W. K., Craine, J. M., Dobrin, B. H., Duarte, L., Durka, W., Elser, J., Esser, G., Estiarte, M., Fagan, W. F., Fang, J., Fernández-Méndez, F., Fidelis, A., Finegan, B., Flores, O., Ford, H., Frank, D., Freschet, G. T., Fyllas, N. M., Gallagher, R. V., Green, W. A., Gutierrez, A. G., Hickler, T., Higgins, S. I., Hodgson, J. G., Jalili, A., Jansen, S., Joly, C. A., Kerkhoff, A. J., Kirkup, D., Kitajima, K., Kleyer, M., Klotz, S., Knops, J. M. H., Kramer, K., Kühn, I., Kurokawa, H., Laughlin, D., Lee, T. D., Leishman, M., Lens, F., Lenz, T., Lewis, S.L., Lloyd, J., Llusià, J., Louault, F., Ma, S., Mahecha, M. D., Manning, P., Massad, T., Medlyn, B. E., Messier, J., Moles, A. T., Müller, S. C., Nadrowski, K., Naeem, S., Niinemets, Ü., Nöllert, S., Nüske, A., Ogaya, R., Oleksyn, J., Onipchenko, V. G., Onoda, Y., Ordoñez, J., Overbeck, G., Ozinga, W. A., Patiño, S., Paula, S., Pausas, J. G., Peñuelas, J., Phillips, O. L., Pillar, V., Poorter, H., Poorter, L., Poschlod, P., Prinzing, A., Proulx, R., Rammig, A., Reinsch, S., Reu, B., Sack, L., Salgado-Negret, B., Sardans, J., Shiodera, S., Shipley, B., Siefert, A., Sosinski, E., Soussana, J. F., Swaine, E., Swenson, N., Thompson, K., Thornton, P., Waldram, M., Weiher, E., White, M., White, S., Wright, S.J., Yguel, B., Zaehle, S., Zanne, A. E., and Wirth, C.: TRY – a global database of plant traits, Glob. Change Biol., 17, 2905–2935, doi:10.1111/j.1365-2486.2011.02451.x, 2011.

Kimball, J. S., White, M. A., and Running, S. W.: BIOME-BGC simulations of stand hydrologic processes for BOREAS, J. Geophys. Res., 102, 29043–29051, doi:10.1029/97JD02235, 1997.

Knorr, W. and Kattge, J.: Inversion of terrestrial ecosystem model parameter values against eddy covariance measurements by Monte Carlo sampling, Glob. Change Biol., 11, 1333–1351, doi:10.1111/j.1365-2486.2005.00977.x, 2005.

Korol, R. L., Milner, K. S., and Running, S. W.: Testing a mechanistic model for predicting stand and tree growth, Forest Sci., 42, 139–153, 1996.

Kulkarni, M. V., Burgin, A. J., Groffman, P. M., and Yavitt, J. B.: Direct flux and N-15 tracer methods for measuring denitrification in forest soils, Biogeochemistry, 117, 359–373, doi:10.1007/s10533-013-9876-7, 2014.

Lagergren, F., Grelle, A., Lankreijer, H., Mölder, M., and Lindroth, A.: Current carbon balance of the forested area in Sweden and its sensitivity to global change as simulated by Biome-BGC, Ecosystems, 9, 894–908, doi:10.1007/s10021-005-0046-1, 2006.

Leuning, R.: A critical appraisal of a combined stomatal-photosynthesis model for C3 plants, Plant. Cell Environ., 18, 339–355, doi:10.1111/j.1365-3040.1995.tb00370.x, 1995.

Liu, H. P., Peters, G., and Foken, T.: New equations for sonic temperature variance and buoyancy heat flux with an omnidirectional sonic anemometer, Bound.-Lay Meteorol., 100, 459–468, doi:10.1023/A:1019207031397, 2001.

Lombardozzi, D. L., Bonan, G. B., Smith, N. G., Dukes, J. S., and Fisher, R. A.: Temperature acclimation of photosynthesis and respiration: a key uncertainty in the carbon cycle-climate feedback, Geophys. Res. Lett., 42, 8624–8631, doi:10.1002/2015GL065934, 2015.

Ma, S., Churkina, G., Wieland, R., and Gessler, A.: Optimization and evaluation of the ANTHRO-BGC model for winter crops in Europe, Ecol. Model., 222, 3662–3679, doi:10.1016/j.ecolmodel.2011.08.025, 2011.

Ma, S., Acutis, A., Barcza, Z., Touhami, H. B., Doro, L., Hidy, D., Köchy, M., Minet, J., Lellei-Kovács, E., Perego, A., Rolinski, A., Ruget, F., Seddaiu, G., Wu, L., and Bellocchi, G.: The grassland model intercomparison of the MACSUR (Modelling European Agriculture with Climate Change for Food Security) European knowledge hub, in: Proceedings of the 7th International Congress on Environmental Modelling and Software, edited by: Ames, D. P., Quinn, N. W. T., and Rizzoli, A. E., San Diego, California, USA, 2014.

Marjanović, H., Alberti, G., Balogh, J., Czóbel, S., Horváth, L., Jagodics, A., Nagy, Z., Ostrogović, M. Z., Peressotti, A., and Führer, E.: Measurements and estimations of biosphere-atmosphere exchange of greenhouse gases – Grasslands, in: Atmospheric Greenhouse Gases: The Hungarian Perspective, edited by: Haszpra, L., Springer, Dordrecht – Heidelberg – London – New York, 121–156, doi:10.1007/978-90-481-9950-1_7, 2011a.

Marjanović, H., Ostrogović, M. Z., Alberti, G., Balenović, I., Paladinić, E., Indir, K., Peresotti, A., and Vuletić, D.: Carbon dynamics in younger stands of pedunculate oak during two vegetation periods, Šum. list special issue, 135, 59–73, 2011b (in Croatian with English summary).

Martre, P., Wallach, D., Asseng, S., Ewert, F., Jones, J. W., Rotter, R. P., Boote, K. J., Ruane, A. C., Thorburn, P. J., Cammarano, D., Hatfield, J. L., Rosenzweig, C., Aggarwal, P. K., Angulo, C., Basso, B., Bertuzzi, P., Biernath, C., Brisson, N., Challinor, A. J., Doltra, J., Gayler, S., Goldberg, R., Grant, R. F., Heng, L., Hooker, J., Hunt, L. A., Ingwersen, J., Izaurralde, R. C., Kersebaum, K. C., Müller, C., Kumar, S. N., Nendel, C., O'leary, G., Olesen, J. E., Osborne, T. M., Palosuo, T., Priesack, E., Ripoche, D., Semenov, M. A., Shcherback, I., Steduto, P., Stöckle, C. O., Stratonovitch, P., Streck, T., Supit, I., Tao, F., Travasso, M., Waha, K., White, J. W., and Wolf, J.: Multimodel ensembles of wheat growth: many models are better than one, Glob. Change Biol., 21, 911–925, doi:10.1111/gcb.12768, 2015.

Maselli, F., Chiesi, M., Brilli, L., and Moriondo, M.: Simulation of olive fruit yield in Tuscany through the integration of remote sensing and ground data, Ecol. Model., 244, 1–12, doi:10.1016/j.ecolmodel.2012.06.028, 2012.

Massman, W. J.: The attenuation of concentration fluctuations in turbulent flow through a tube, J. Geophys. Res., 96, 15269–15273, doi:10.1029/91JD01514, 1991.

Mayer, B.: Hydropedological relations in the region of lowland forests of Pokupsko basin, Radovi Šumarskog instituta Jastrebarsko, 31, 37–89, 1996 (in Croatian with English summary).

Medlyn, B. E., Dreyer, E., Ellsworth, D., Forstreuter, M., Harley, P. C., Kirschbaum, M. U. F., Le Roux, X., Montpied, P., Strassemeyer, J., Walcroft, A., Wang, K., and Loustau, D.: Temperature response of parameters of a biochemically based model of photosynthesis. II. A review of experimental data, Plant. Cell Environ., 25, 1167–1179, doi:10.1046/j.1365-3040.2002.00891.x, 2002.

Merganičová, K., Pietsch, S. A., and Hasenauer, H.: Testing mechanistic modeling to assess impacts of biomass removal, Forest Ecol. Manag., 207, 37–57, doi:10.1016/j.foreco.2004.10.017, 2005.

Moore, C. J.: Frequency-response corrections for eddy-correlation systems, Bound.-Lay. Meteorol., 37, 17–35, doi:10.1007/BF00122754, 1986.

Morecroft, M. D. and Roberts, J. M.: Photosynthesis and stomatal conductance of mature canopy Oak and Sycamore trees throughout the growing season, Funct. Ecol., 13, 332–342, 1999.

Mu, Q., Zhao, M., Running, S. W., Liu, M., and Tian, H.: Contribution of increasing CO_2 and climate change to the carbon cycle in China's ecosystems, J. Geophys. Res.-Biogeo., 113, G01018, doi:10.1029/2006JG000316, 2008.

Nagy, Z., Pintér, K., Czóbel, S., Balogh, J., Horváth, L., Fóti, S., Barcza, Z., Weidinger, T., Csintalan, Z., Dinh, N. Q., Grosz, B., and Tuba, Z.: The carbon budget of semi-arid grassland in a wet and a dry year in Hungary, Agr. Ecosyst. Environ., 121, 21–29, doi:10.1016/j.agee.2006.12.003, 2007.

Nagy, Z., Barcza, Z., Horváth, L., Balogh, J., Hagyó, A., Káposztás, N., Grosz, B., Machon, A., and Pintér, K.: Measurements and estimations of biosphere-atmosphere exchange of greenhouse gases – Grasslands, in: Atmospheric Greenhouse Gases: The Hungarian Perspective, edited by: Haszpra, L., 91–120, Springer, Dordrecht – Heidelberg – London – New York, 2011.

Nakai, T., van der Molen, M. K., Gash, J. H. C., and Kodama, Y: Correction of sonic anemometer angle of attack errors, Agr. Forest Meteorol., 136, 19–30, doi:10.1016/j.agrformet.2006.01.006, 2006.

Nemani, R. R. and Running, S. W.: Testing a theoretical climate-soil-leaf area hydrologic equilibrium of forests using satellite data and ecosystem simulation, Agr. Forest Meteorol., 44, 245–260, doi:10.1016/0168-1923(89)90020-8, 1989.

Olin, S., Schurgers, G., Lindeskog, M., Wårlind, D., Smith, B., Bodin, P., Holmér, J., and Arneth, A.: Modelling the response of yields and tissue C : N to changes in atmospheric CO_2 and

N management in the main wheat regions of western Europe, Biogeosciences, 12, 2489–2515, doi:10.5194/bg-12-2489-2015, 2015.

Ostrogović, M. Z.: Carbon stocks and carbon balance of an even-aged pedunculate oak (Quercus robur L.) forest in Kupa river basin, doctoral thesis, Faculty of forestry, University of Zagreb, 2013 (in Croatian with English summary).

Petritsch, R., Hasenauer, H., and Pietsch, S. A.: Incorporating forest growth response to thinning within biome-BGC, Forest Ecol. Manag., 242, 324–336, doi:10.1016/j.foreco.2007.01.050, 2007.

Pietsch, S. A., Hasenauer, H., Kucera, J., and Cermák, J.: Modeling effects of hydrological changes on the carbon and nitrogen balance of oak in floodplains, Tree Physiol., 23, 735–746, 2003.

Reichstein, M., Falge, E., Baldocchi, D., Papale, D., Aubinet, M., Berbigier, P., Bernhofer, C., Buchmann, N., Gilmanov, T., Granier, A., Grunwald, T., Havrankova, K., Ilvesniemi, H., Janous, D., Knohl, A., Laurila, T., Lohila, A., Loustau, D., Matteucci, G., Meyers, T., Miglietta, F., Ourcival, J. M., Pumpanen, J., Rambal, S., Rotenberg, E., Sanz, M., Tenhunen, J., Seufert, G., Vaccari, F., Vesala, T., Yakir, D., and Valentini, R.: On the separation of net ecosystem exchange into assimilation and ecosystem respiration: review and improved algorithm, Glob. Change Biol., 11, 1424–1439, doi:10.1111/j.1365-2486.2005.001002.x, 2005.

Ritchie, J. T.: Soil water balance and plant water stress, in: Understanding Options for Agricultural Production, edited by: Tsuji, G. Y., Hoogenboom, G., and Thornton, P. E., Kluwer Academic Publishers, The Netherlands, 41–54, 1998.

Running, S. W. and Coughlan, J. C.: A general model of forest ecosystem processes for reginonal applications I. Hydrologic balance, canopy gas exchange and primary production processes, Ecol. Model., 42, 125–154, doi:10.1016/0304-3800(88)90112-3, 1988.

Running, S. W. and Gower, S. T.: FOREST-BGC, A general model of forest ecosystem processes for regional applications. II. Dynamic carbon allocation and nitrogen budgets, Tree Physiol., 9, 147–160, doi:10.1093/treephys/9.1-2.147, 1991.

Running, S. W. and Hunt, E. R. J.: Generalization of a forest ecosystem process model for other biomes, BIOME-BGC, and an application for global-scale models, in: Scaling Physiological Processes: Leaf to Globe, edited by: Ehleringer, J. R. and Field, C., Academic Press, San Diego, 141–158, 1993.

Sándor, R. and Fodor, N.: Simulation of soil temperature dynamics with models using different concepts, Sci. World J., 2012, 1–8, doi:10.1100/2012/590287, 2012.

Sándor, R., Ma, S., Acutis, M., Barcza, Z., Ben Touhami, H., Doro, L., Hidy, D., Köchy, M., Lellei-Kovács, E., Minet, J., Perego, A., Rolinski, S., Ruget, F., Seddaiu, G., Wu, L., and Bellocchi, G.: Uncertainty in simulating biomass yield and carbon-water fluxes from grasslands under climate change, Advances in Animal Biosciences, 6, 49–51, doi:10.1017/S2040470014000545, 2015.

Sándor, R., Barcza, Z., Hidy, D., Lellei-Kovács, E., Ma, S., and Bellocchi, G.: Modelling of grassland fluxes in Europe: evaluation of two biogeochemical models, Agr. Ecosyst. Environ., 215, 1–19, doi:10.1016/j.agee.2015.09.001, 2016.

Schmid, S., Zierl, B., and Bugmann, H.: Analyzing the carbon dynamics of central European forests: comparison of Biome-BGC simulations with measurements, Reg. Environ. Chang., 6, 167–180, doi:10.1007/s10113-006-0017-x, 2006.

Schulze, E. D., Luyssaert, S., Ciais, P., Freibauer, A., Janssens, I. A., Soussana, J. F., Smith, P., Grace, J., Levin, I., Thiruchittampalam, B., Heimann, M., Dolman, A. J., Valentini, R., Bousquet, P., Peylin, P., Peters, W., Rödenbeck, C., Etiope, G., Vuichard, N., Wattenbach, M., Nabuurs, G. J., Poussi, Z., Nieschulze, J., Gash, J. H., and CarboEurope Team: Importance of methane and nitrous oxide for Europe's terrestrial greenhouse-gas balance, Nat. Geosci., 2, 842–850, doi:10.1038/ngeo686, 2009.

Schwalm, C. R., Williams, C. A., Schaefer, K., Anderson, R., Arain, M. A., Baker, I., Barr, A., Black, T. A., Chen, G., Chen, J. M., Ciais, P., Davis, K. J., Desai, A., Dietze, M., Dragoni, D., Fischer, M. L., Flanagan, L. B., Grant, R., Gu, L., Hollinger, D., Izaurralde, R. C., Kucharik, C., Lafleur, P., Law, B. E., Li, L., Li, Z., Liu, S., Lokupitiya, E., Luo, Y., Ma, S., Margolis, H., Matamala, R., McCaughey, H., Monson, R. K., Oechel, W. C., Peng, C., Poulter, B., Price, D. T., Riciutto, D. M., Riley, W., Sahoo, A. K., Sprintsin, M., Sun, J., Tian, H., Tonitto, C., Verbeeck, H., and Verma, S. B.: A model-data intercomparison of CO_2 exchange across North America: Results from the North American Carbon Program site synthesis, J. Geophys. Res., 115, G00H05, doi:10.1029/2009JG001229, 2010.

Schwalm, C. R., Huntinzger, D. N., Fisher, J. B., Michalak, A. M., Bowman, K., Cias, P., Cook, R., El-Masri, B., Hayes, D., Huang, M., Ito, A., Jain, A., King, A.W., Lei, H., Liu, J., Lu, C., Mao, J., Peng, S., Poulter, B., Ricciuto, D., Schaefer, K., Shi, X., Tao, B., Tian, H., Wang, W., Wei, Y., Yang, J., and Zeng, N.: Toward "optimal" integration of terrestrial biosphere models, Geophys. Res. Lett., 42, 4418–4428, doi:10.1002/2015GL064002, 2015.

Smith, N. G. and Dukes, J. S.: Plant respiration and photosynthesis in global-scale models: Incorporating acclimation to temperature and CO_2, Glob. Change Biol., 19, 45–63, doi:10.1111/j.1365-2486.2012.02797.x, 2012.

Suyker, A. E., Verma, S. B., and Burba, G. G.: Interannual variability in net CO_2 exchange of a native tallgrass prairie, Glob. Change Biol., 9, 255–265, doi:10.1046/j.1365-2486.2003.00567.x, 2003.

Suyker, A. E., Verma, S. B., Burba, G. G., Arkebauer, T. J., Walters, D. T., and Hubbard, K. G.: Growing season carbon dioxide exchange in irrigated and rainfed maize, Agr. Forest Meteorol., 124, 1–13, doi:10.1016/j.agrformet.2004.01.011, 2004.

Tatarinov, F. A. and Cienciala, E.: Application of BIOME-BGC model to managed forests, Forest Ecol. Manag., 237, 267–279, doi:10.1016/j.foreco.2006.09.085, 2006.

Thomas, R. Q., Bonan, G. B., and Goodale, C. L.: Insights into mechanisms governing forest carbon response to nitrogen deposition: a model–data comparison using observed responses to nitrogen addition, Biogeosciences, 10, 3869–3887, doi:10.5194/bg-10-3869-2013, 2013.

Thornton, P., Law, B., Gholz, H. L., Clark, K. L., Falge, E., Ellsworth, D., Goldstein, A., Monson, R., Hollinger, D., Falk, M., Chen, J., and Sparks, J.: Modeling and measuring the effects of disturbance history and climate on carbon and water budgets in evergreen needleleaf forests, Agr. Forest Meteorol., 113, 185–222, doi:10.1016/S0168-1923(02)00108-9, 2002.

Thornton, P. E.: Regional ecosystem simulation: Combining surface- and satellite-based observations to study linkages between terrestrial energy and mass budgets, The University of Montana, 1998.

Thornton, P. E.: User's Guide for Biome-BGC, Version 4.1.1., available at: ftp://daac.ornl.gov/data/model_archive/BIOME_BGC/biome_bgc_4.1.1/comp/bgc_users_guide_411.pdf (last access: April 2016), 2000.

Thornton, P. E. and Rosenbloom, N. A.: Ecosystem model spin-up: Estimating steady state conditions in a coupled terrestrial carbon and nitrogen cycle model, Ecol. Model., 189, 25–48, doi:10.1016/j.ecolmodel.2005.04.008, 2005.

Thornton, P. E., Lamarque, J. F., Rosenbloom, N. A., and Mahowald, N. M.: Influence of carbon-nitrogen cycle coupling on land model response to CO_2 fertilization and climate variability, Global Biogeochem. Cy., 21, GB4018, doi:10.1029/2006GB002868, 2007.

Tjoelker, M. G., Oleksyn, J., and Reich, P. B.: Modelling respiration of vegetation: evidence for a general temperature-dependent Q10, Glob. Change Biol., 7, 223–230, doi:10.1046/j.1365-2486.2001.00397.x, 2001.

Trusilova, K. and Churkina, G.: The response of the terrestrial biosphere to urbanization: land cover conversion, climate, and urban pollution, Biogeosciences, 5, 1505–1515, doi:10.5194/bg-5-1505-2008, 2008.

Trusilova, K., Trembath, J., and Churkina, G.: Parameter estimation and validation of the terrestrial ecosystem model Biome-BGC using eddy-covariance flux measurements, Technical Report 16, MPI for Biogeochemistry, Jena, 2009.

Ťupek, B., Zanchi, G., Verkerk, P. J., Churkina, G., Viovy, N., Hughes, J. K., and Lindner, M.: A comparison of alternative modelling approaches to evaluate the European forest carbon fluxes, Forest Ecol. Manag., 260, 241–251, doi:10.1016/j.foreco.2010.01.045, 2010.

Turner, D. P., Ritts, W. D., Law, B. E., Cohen, W. B., Yang, Z., Hudiburg, T., Campbell, J. L., and Duane, M.: Scaling net ecosystem production and net biome production over a heterogeneous region in the western United States, Biogeosciences, 4, 597–612, doi:10.5194/bg-4-597-2007, 2007.

Ueyama, M., Ichii, K., Hirata, R., Takagi, K., Asanuma, J., Machimura, T., Nakai, Y., Ohta, T., Saigusa, N., Takahashi, Y., and Hirano, T.: Simulating carbon and water cycles of larch forests in East Asia by the BIOME-BGC model with AsiaFlux data, Biogeosciences, 7, 959–977, doi:10.5194/bg-7-959-2010, 2010.

van Bodegom, P. M., Douma, J. C., Witte, J. P. M., Ordonez, J. C., Bartholomeus, R. P., and Aerts, R.: Going beyond limitations of plant functional types when predicting global ecosystem–atmosphere fluxes: exploring the merits of traits-based approaches, Global Ecol. Biogeogr., 21, 625–636, doi:10.1111/j.1466-8238.2011.00717.x, 2012.

van der Molen, M. K., Gash, J. H. C., and Elbers, J. A.: Sonic anemometer (co)sine response and flux measurement – II. The effect of introducing an angle of attack dependent calibration, Agr. Forest Meteorol., 122, 95–109, 2004.

van der Molen, M. K., Dolman, A. J., Ciais, P., Eglin, T., Gobron, N., Law, B. E., Meir, P., Peters, W., Phillips, O. L., Reichstein, M., Chen, T., Dekker, S. C., Doubková, M., Friedl, M. A., Jung, M., , van den Hurk, B. J. J. M., de Jeu, R. A. M., Kruijt, B., Ohta, T., Rebel, K. T., Plummer, S., Seneviratne, S. I., Sitch, S., Teuling, A. J., van der Werf, G. R., and Wang, G.: Drought and ecosystem carbon cycling, Agr. Forest Meteorol., 151, 765–773, doi:10.1016/j.agrformet.2011.01.018, 2011.

Verma, S. B., Dobermann, A., Cassman, K. G., Walters, D. T., Knops, J. M. N., Arkebauer, T. J., Suyker, A. E., Burba, G., Amos, B., Yang, H., Ginting, D., Hubbard, K., Gitleson, A. A., and Walter-Shea, E. A.: Annual carbon dioxide exchange in irrigatedrainfed maize based agroecosystems, Agr. Forest Meteorol., 131, 77–96, doi:10.1016/j.agrformet.2005.05.003, 2005.

Vetter, M., Wirth, C., Böttcher, H., Churkina, G., Schulze, E.-D., Wutzler, T., and Weber, G.: Partitioning direct and indirect human-induced effects on carbon sequestration of managed coniferous forests using model simulations and forest inventories, Glob. Change Biol., 11, 810–827, doi:10.1111/j.1365-2486.2005.00932.x, 2005.

Vetter, M., Churkina, G., Jung, M., Reichstein, M., Zaehle, S., Bondeau, A., Chen, Y., Ciais, P., Feser, F., Freibauer, A., Geyer, R., Jones, C., Papale, D., Tenhunen, J., Tomelleri, E., Trusilova, K., Viovy, N., and Heimann, M.: Analyzing the causes and spatial pattern of the European 2003 carbon flux anomaly using seven models, Biogeosciences, 5, 561–583, doi:10.5194/bg-5-561-2008, 2008.

Vickers, D. and Mahrt, L.: Quality control and flux sampling problems for tower and aircraft data, J. Atmos. Ocean. Tech., 14, 512–526, doi:10.1175/1520-0426(1997)014<0512:QCAFSP>2.0.CO;2, 1997.

Vitousek, P., Edin, L. O., Matson, P. A., Fownes, J. H., and Neff, J.: Within-system element cycles, input-output budgets, and nutrient limitations, in: Success, Limitations, and Frontiers in Ecosystem Science, edited by: Pace, M. and Groffman, P., Springer, New York, 432–451, 1998.

Vitousek, P. M., Fahey, T., Johnson, D. W., and Swift, M. J.: Element interactions in forest ecosystems: succession, allometry and input-output budgets, Biogeochemistry, 5, 7–34, doi:10.1007/BF02180316, 1988.

Wang, Q., Watanabe, M., and Ouyang, Z.: Simulation of water and carbon fluxes using BIOME-BGC model over crops in China, Agr. Forest Meteorol., 131, 209–224, doi:10.1016/j.agrformet.2005.06.002, 2005.

Webb, E. K., Pearman, G. I., and Leuning, R.: Correction of flux measurements for density effects due to heat and water-vapor transfer, Q. J. Roy. Meteor. Soc., 106, 85–100, doi:10.1002/qj.49710644707, 1980.

White, A., Melvin, G. R., Cannell, A., and Friend, D.: Climate change impacts on ecosystems and the terrestrial carbon sink: a new assessment, Global Environ. Change, 9, 21–30, doi:10.1016/S0959-3780(99)00016-3, 1999.

White, M., Thornton, P. E., Running, S. W., and Nemani, R. R.: Parameterization and sensitivity analysis of the BIOME–BGC terrestrial ecosystem model: Net primary production controls, Earth Interact., 4, 1–85, doi:10.1175/1087-3562(2000)004<0003:PASAOT>2.0.CO;2, 2000.

Wilczak, J. M., Oncley, S. P., and Stage, S. A.: Sonic anemometer tilt correction algorithms, Bound.-Lay. Meteor., 99, 127–150, doi:10.1023/A:1018966204465, 2001.

Williams, J. R.: Runoff and water erosion, in Modeling plant and soil systems, Agronomy Monograph nr. 31, edited by: Hanks, R. J. and Ritchie, J. T., American Society of Agronomy, Madison, Wisconsin, USA, 439–455, 1991.

Williams, M., Richardson, A. D., Reichstein, M., Stoy, P. C., Peylin, P., Verbeeck, H., Carvalhais, N., Jung, M., Hollinger, D. Y., Kattge, J., Leuning, R., Luo, Y., Tomelleri, E., Trudinger, C. M.,

and Wang, Y.-P.: Improving land surface models with FLUXNET data, Biogeosciences, 6, 1341–1359, doi:10.5194/bg-6-1341-2009, 2009.

Woodrow, I. E. and Berry, J. A.: Enzymatic regulation of photosynthetic CO_2 fixation in C3 plants, Annu. Rev. Plant Phys., 39, 533–594, doi:10.1146/annurev.pp.39.060188.002533, 1988.

WRB: World Reference Base for Soil Resources (WRB), World Soil Resources Reports No. 103, IX+128 pp., ISSS, ISRIC and United Nations Food and Agriculture Organization (FAO), Rome, 2006.

Yi, C., Ricciuto, D., Li, R., Wolbeck, J., Xu, X., Nilsson, M., Aires, L., Albertson, J. D., Amman, C., Arain, M. A., de Araujo, A. C., Aubinet, M., Aurela, M., Barcza, Z., Barr, A., Berbigier, P., Beringer, J., Bernhofer, C., Black, A. T., Bolstad, P. V., Bosveld, F. C., Broadmeadow, M. S. J., Buchmann, N., Burns, S. P., Cellier, P., Chen, J., Chen, J., Ciais, P., Clement, R., Cook, B. D., Curtis, P. S., Dail, D. B., Dellwik, E., Delpierre, N., Desai, A. R., Dore, S., Dragoni, D., Drake, B. G., Dufrêne, E., Dunn, A., Elbers, J., Eugster, W., Falk, M., Feigenwinter, C., Flanagan, L. B., Foken, T., Frank, J., Fuhrer, J., Gianelle, D., Golstein, A., Goulden, M., Granier, A., Grunwald, T., Gu, L., Guo, H., Hammerle, A., Han, S., Hanan, N. P., Haszpra, L., Heinesch, B., Helfter, C., Hendriks, D., Hutley, L. B., Ibrom, A., Jacobs, C., Johansson, T., Jongen, M., Katul, G., Kiely, G., Klumpp, K., Knohl, A., Kolb, T., Kutsch, W. L., Lafleur, P., Laurila, T., Leuning, R., Lindroth, A., Liu, H., Loubet, B., Manca, G., Marek, M., Margolis, H. A., Martin, T. A., Massman, W. J., Matamala, R., Matteucci, G., McCaughey, H., Merbold, L., Meyers, T., Migliavacca, M., Miglietta, F., Misson, L., Molder, M., Moncrieff, J., Monson, R. K., Montagnani, L., Montes-Helu, M., Moors, E., Moureaux, C., et al.: Climate control of terrestrial carbon exchange across biomes and continents, Environ. Res. Lett., 5, 034007, doi:10.1088/1748-9326/5/3/034007, 2010.

Zheng, D., Raymond, H., and Running, S. W.: A daily soil temperature model based on air temperature and precipitation for continental applications, Clim. Res., 2, 183–191, doi:10.3354/cr002183, 1993.

Corrigendum to "Terrestrial Ecosystem Process Model Biome-BGCMuSo v4.0: Summary of improvements and new modeling possibilities" [GMD-9-4405-2016]

Dóra Hidy[1], Zoltán Barcza[2], Hrvoje Marjanović[3], Maša Zorana Ostrogović Sever[3], Laura Dobor[2], Györgyi Gelybó[4], Nándor Fodor[5], Krisztina Pintér[1], Galina Churkina[6], Steven Running[7], Peter Thornton[8], Gianni Bellocchi[9], László Haszpra[10,13], Ferenc Horváth[11], Andrew Suyker[12], Zoltán Nagy[1]

[1] MTA-SZIE Plant Ecology Research Group, Szent István University, Páter K. u.1., H-2103 Gödöllő, Hungary
[2] Department of Meteorology, Eötvös Loránd University, Pázmány P. sétány 1/A., H-1117 Budapest, Hungary
[3] Croatian Forest Research Institute, Department for Forest Management and Forestry Economics, Cvjetno naselje 41, 10450 Jastrebarsko, Croatia
[4] Institute for Soil Sciences and Agricultural Chemistry, Centre for Agricultural Research, Hungarian Academy of Sciences, Herman O. út 15., H-1163 Budapest, Hungary
[5] Agricultural Institute, Centre for Agricultural Research, Hungarian Academy of Sciences, Brunszvik u. 2., H-2462
Martonvásár, Hungary
[6] Institute for Advanced Sustainability Studies e.V., Berliner Strasse 130, D-14467 Potsdam, Germany
[7] Numerical Terradynamic Simulation Group, Department of Ecosystem and Conservation Sciences University of Montana, Missoula, MT 59812 USA
[8] Climate Change Science Institute / Environmental Sciences Division, Oak Ridge National Laboratory, Oak Ridge, TN 37831-6335, USA
[9] UREP, INRA, 63000 Clermont-Ferrand, France
[10] Hungarian Meteorological Service, H-1675 Budapest, P.O.Box 39, Hungary
[11] Institute of Ecology and Botany, Centre for Ecological Research, Hungarian Academy of Sciences, Alkotmány u. 2-4., H-2163 Vácrátót, Hungary
[12] School of Natural Resources, University of Nebraska-Lincoln, 806 Hardin Hall, Lincoln, Nebraska 68588, USA
[13] Geodetic and Geophysical Institute, MTA Research Centre for Astronomy and Earth Sciences, H-9400 Sopron, Csatkai Endre utca 6-8., Hungary

Correspondence to: Dóra Hidy (dori.hidy@gmail.com)

Table 2. Default values of parameters in BBGCMuSo for different soil types. Soil types are identified based on the used-defined sand, silt and clay fraction of the soil layers based on the soil triangle method.

	SAND	LOAMY SAND	SANDY LOAM	LOAM	SILT LOAM	SILT	SANDY CLAY LOAM	CLAY LOAM	SILT CLAY LOAM	SANDY CLAY	SILT CLAY	CLAY
B	3.45	4.11	5.26	6.12	5.39	4.02	7.63	7.71	8.56	9.22	10.45	12.46
SWC_{sat}	0.4	0.42	0.44	0.46	0.48	0.49	0.5	0.505	0.51	0.515	0.52	0.525
SWC_{fc}	0.155	0.19	0.25	0.31	0.36	0.38	0.39	0.405	0.42	0.435	0.445	0.46
SWC_{wp}	0.03	0.05	0.09	0.13	0.17	0.19	0.205	0.22	0.24	0.26	0.275	0.29
BD	1.60	1.58	1.56	1.54	1.52	1.5	1.48	1.46	1.44	1.42	1.4	1.38
RCN	50	52	54	56	58	60	62	64	66	68	70	72